Journal of Hazardous Materials 470 (2024) 134230

Contents lists available at ScienceDirect

Journal of Hazardous Materials

journal homepage: www.elsevier.com/locate/jhazmat

# Antimony release and volatilization from organic-rich and iron-rich submerged soils

J.N. Caplette [a,b,*], S.C. Wilson [c], A. Mestrot [a,*]

[a] Institute of Geography, University of Bern, Switzerland
[b] Minnow Aquatic Environmental Services, Toronto, Canada
[c] School of Environmental and Rural Science, University of New England, Armidale, NSW, Australia

## HIGHLIGHTS

- Both soil types released environmentally relevant concentrations of Sb into the porewaters.
- Waterlogging soils promotes the release of Sb into porewaters.
- Soil-type influences the release and attenuation of Sb in porewaters.
- Volatile Sb was produced from both soils, with more produced in the organic-rich soil than the iron-rich soil.

## GRAPHICAL ABSTRACT

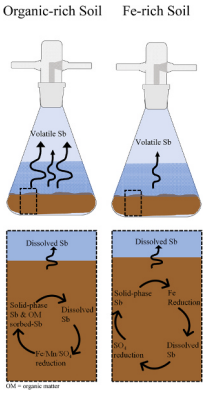


## ARTICLE INFO

*Keywords:*
Wetland
Sulfate reduction
Flooding
Speciation
Methylation

## ABSTRACT

Antimony (Sb) is an poorly understood, increasingly common pollutant, especially in soils susceptible to waterlogging. We investigated the impact of waterlogging on Sb release, methylation, and volatilization from an organic-rich wetland soil and an iron (Fe)-rich floodplain soil in a 27-day microcosm experiment. The release of Sb into the porewaters of the organic-rich soil was environmentally relevant and immediate with waterlogging (3.2 to 3.5 mg $L^{-1}$), and likely associated with a complex interplay of sulfide precipitation, sorption with organic matter and manganese (Mn) (oxyhydr)oxides in the soil. The release of Sb from the Fe-rich soil was likely associated with Fe-(oxyhydr)oxide reduction and immobilized due to co-precipitation with Fe-sulfides or as Sb-sulfides. Volatile Sb was produced from the soils after waterlogging. The organic-rich soil produced more volatile Sb (409 to 835 ng $kg_{soil}^{-1}$), but the Fe-rich soil volatilized Sb more efficiently. The negligible association of Sb volatilization with soil parameters indicates a more complex underlying, potentially microbial, mechanism and that antimony volatilization could be ubiquitous and not dependent on specific soil properties. Future works should investigate the microbial and physiochemical drivers of Sb volatilization in soils as it may be an environmentally relevant part of the biogeochemical cycle.

* Corresponding authors at: Institute of Geography, University of Bern, Switzerland.
*E-mail addresses:* jaime.caplette@minnow.ca (J.N. Caplette), adrien.mestrot@giub.unibe.ch (A. Mestrot).

https://doi.org/10.1016/j.jhazmat.2024.134230
Received 21 January 2024; Received in revised form 1 April 2024; Accepted 4 April 2024
Available online 5 April 2024

## 1. Introduction

With its increased use as a flame retardant, additive in polyethylene terephthalate (PET), munitions, batteries, and applications in green energy, antimony (Sb) is one of thirty-five critical minerals [1,2] and has become more of an environmental concern over the past decades [3-5]. Antimony is classified as a priority pollutant of interest by the US-EPA and EU and some species are potentially carcinogenic [6,7]. Thus, its fate in the environment and impact on water and soil quality, health, and food safety necessitates investigation in regions with elevated Sb concentrations.

Over the past decades, there has been a considerable increase in research on Sb behavior and speciation in the environment. However, these efforts have mostly focused on well-drained aerobic sediments and soils [8-12]. In wetland soils, Sb behavior has received much less attention [3,8,13–15], although wetlands constitute 700 to 1000 Mha of the Earth [16]. Wetland and floodplain soils are influenced by regional hydrologic conditions and are either completely anoxic or periodically anoxic. Consequently, the fate of Sb, which is a redox-sensitive element, is likely influenced.

The redox potential ($E_h$) and pH of soils and sediments are major drivers of Sb behavior in the environment. The speciation of inorganic Sb is dominated by the trivalent Sb species, $Sb^{III}$, $Sb(OH)_3$, in reducing conditions and by the anionic pentavalent species, $Sb^{V}$, $Sb(OH)_6^-$ in aerobic conditions [12,17,18]. While $Sb^{III}$ does not exhibit pH-dependent binding under normal environmental conditions, $Sb^{V}$ is more strongly bound to goethite and ferrihydrite at a pH below 7 [19-21]. The redox chemistry of iron (Fe), manganese (Mn) and sulfur (S) in wetlands and floodplains strongly influence Sb fate in the environment by reductive dissolution of host-phases and by the formation of complexes and/or co-precipitates [22-25].

Restricted oxygen diffusion in soils and sediments induced by waterlogging and fluctuating water tables influence metal(loid) mobility by shifting microbial communities to alternative electron acceptors for energy, such as $Mn^{IV}$ and $Fe^{III}$-(oxyhydr)oxides coupled to the oxidation of organic C [16,22,23,26–28]. Sb typically forms inner-sphere complexes with $Fe^{III}$- and $Mn^{IV}$-(oxyhydr)oxides in soils and sediments, and periodic or permanent waterlogging can induce Sb release by reductive dissolution of the host phases [26,27,29,30]. Soluble Sb can be subsequently sequestered with waterlogging due to stronger adsorption of $Sb^{III}$ to Fe-phases in the soil [23,29], immobilized by sulfides [3,31,32], or $Fe^{II}$ catalyzed $Fe^{III}$-phase transformations at neutral conditions, which incorporate $Sb^{V}$ into authigenic $Fe^{III}$-phases (e.g., goethite and feroxyhyte) [33-35].

Microbial sulfate ($SO_4^{2-}$) reduction can produce reduced sulfur species [24,25,36]. The resultant species can co-precipitate with metal(loid)s and reduce their mobility in waterlogged soils and potentially decrease porewater Sb solubility by 1) Sb sorbing with the newly formed sulfides (e.g., mackinawite and pyrite) [32,37] or 2) by forming discrete Sb-sulfides (e.g., amorphous $Sb_2S_3$) and/or complexing with thiol-groups on organic matter [3,13,38-40]. Under neutral conditions, soluble thiolated Sb species may also increase Sb mobility in the environment [41,42].

The influence of organic matter on Sb behavior in the environment is highly variable [39,43–46]. Organic-rich soils, such as peat, may act as important sinks for $Sb^{III}$ in reducing environments by binding Sb to oxygen- and sulfur-bearing functional groups on natural organic matter [38]. For example, Sb complexation with thiol-binding sites in sulfide-reacted peat sorbed up to 98% of $Sb^{III}$, compared to 85% in untreated peat at pH 6 [38]. Dissolved organic matter (DOM) may also enhance Sb mobility by competing for binding sites on $Fe^{III}$- and $Mn^{IV}$-(oxyhydr)oxides [26,47,48] or by forming soluble complexes with low molecular weight organic acids [37,44,45]. Many gaps still exist in our understanding of the different influences on Sb mobility in high organic matter containing soils.

The various influences on Sb speciation will also influence the soluble fraction and the fraction available for microbial transformation. A variety of microorganisms can methylate inorganic Sb [49-53]. These microorganisms are both aerobic [50,51,54–56] and anaerobic [52,53, 57–59]. Soluble methylated pentavalent Sb species (mono-, di- and tri-methylated Sb species (soluble $MMSb^{V}$, $DMSb^{V}$, and $TMSb^{V}$, respectively)) are the products of microbial methylation. The reduced volatile species, trimethylstibine ($(CH_3)_3Sb$), is proposed as the Sb methylation end product [60-63]. Other volatile hydride Sb species (called stibines), such as stibine ($SbH_3$), monomethyl- and dimethyl-stibines, have also been detected in the headspace gases of microbial incubations [53,64,65]. Small volatile Sb yields (<0.03%) in an aerobic prokaryote [66] and the headspace of an anaerobic yeast [50] indicated that the methylation of Sb may be a fortuitous process [50,61, 67]. To date, little is known about the factors that influence Sb methylation and volatilization in soils, even though these transformations may be important on a large scale for Sb cycling in the environment [31].

Methylation of metal(loid)s may influence their mobility. In soils, sediments, and mine tailings, $TMSb^{V}$ was more mobile than monomethylarsenate and dimethylarsenate [68], and when floodplain soils were waterlogged, methylated Sb species were detected in a redox-controlled microcosm (soluble MMSb: 0.09 to 0.61 μg $L^{-1}$ and DMSb: 0.12 to 0.22 μg $L^{-1}$) [14], and up to 7.8 ± 1.1% TMSb was detected in shooting range soil porewaters ([26]. Methylated Sb species have even been detected at higher concentrations than methylated As species in arable, garden, and floodplain soils [69] and pondwater sediment porewaters [70]. In agricultural soils, methylated Sb species were reported to account for up to 2.3% of the total Sb, and MMSb, DMSb, and TMSb were detected, with MMSb (56.0 ± 11.8 μg $kg^{-1}$) the most abundant species [69]. These studies indicate that Sb methylation occurs a variety of environments, where an emphasis of investigations have focused on anaerobic environments.

The detection of volatile Sb from soils has only recently been investigated. Using our newly developed method for volatile Sb capture we demonstrated that volatile Sb was produced from Swiss shooting range [71] and Chinese rice paddy soil microcosms and also directly in the field [31]. We showed in our work that Sb fluxes to the atmosphere may be similar to As fluxes, and could potentially account for a large portion of Sb transfer to the atmosphere [31]. Volatilization of Sb may increase its mobility and toxicity [31,71–74] and certain conditions may favor its release. For example, more volatile Sb was produced in nutrient stimulated cow-dung treated soils than untreated soils [31,71]. Furthermore, the observed correlation between surface water and volatile Sb possibly indicates that volatile Sb may be produced in the surface water of the cow-dung treated soils, and is in contrast to the volatilization of As species [75-77] and other work on volatile Sb [71,78, 79].

As described, organic matter and Fe have an important and contradictory influence on Sb fate in waterlogged soils. This study compares the impact of flooding on Sb release from two different soils with high concentrations of organic matter or Fe (an acidic, organic-rich wetland and an Fe-rich floodplain soil) using microcosm experiments. We also evaluated the influence of waterlogging on Sb volatilization, the release controls of Sb in porewaters, and the formation of TMSb in the waters and soils. The experimental hypothesis was that more volatile Sb would be produced in the organic rich soil but that the high-Fe soil would show a larger fraction of Sb in the solid phase compared to the aqueous phase due to Sb complexing strongly with redox-sensitive host phases.

## 2. Materials and methods

Supra-pur HCl (32%) and $HNO_3$ (69%) produced by distillation (Merck Millipore Inc., Darmstadt, Germany) of p.a. grade acids in a clean-air lab were used throughout the analyses and experiments. Trace-analysis grade (≥ 30%) Supelco $H_2O_2$ was purchased from Sigma Aldrich (Buchs, Switzerland). Ultra-pure water (>18.2 MΩ) from a

Millipore Q-Gard® 2 purification system was used. All glassware and Teflon vials were soaked overnight in 10% $HNO_3$ and rinsed with ultrapure water before use.

Stock Sb solutions were prepared for $Sb^{III}$ from potassium antimony$^{III}$ tartrate (PAT, $C_8H_4K_2O_{12}Sb_2$ x 3 $H_2O$, 99.95%), and TMSb from trimethylantimony$^{V}$ dibromide ($(CH_3)_3SbBr_2$, 98%). The $Sb^{V}$ standard was prepared from potassium hexahydroxoantimonate ($KSb(OH)_6$, 99%). A 10 mg $L^{-1}$ 29-element inorganic inductively coupled plasma (ICP) calibration/quality control standard (Inorganic Ventures, Carl Roth, Karlsruhe, Germany)), and a 1000 mg $L^{-1}$ Sb ICP standard (Sigma-Aldrich, St. Louis, USA) was used for inductively coupled plasma mass spectrometry (ICP-MS) analysis. For speciation analysis, stock solutions of 1000 mg $L^{-1}$ were prepared for $Sb^{III}$ and TMSb and 500 mg $L^{-1}$ for $Sb^{V}$ from their respective salts (Sigma-Aldrich, Buchs, Switzerland). Activated coconut charcoal sorbent tubes (Anasorb CSC, 226–01, surface area of 180 $m^2$, SKC Inc., Eighty Four, USA) were used as Sb traps.

### 2.1. Field site information

Two soils from New South Wales, Australia, were used for the microcosm experiments; an organic soil from the Urunga wetland (GPS coordinates are −30.5051491 N, 153.0112092 E) and a floodplain soil collected from the Macleay River Catchment (MRC, GPS coordinates are −31.0657044 N, 152.9867703 E). Both soils are classified as intertidally saturated Hydrosols [80].

The Urunga wetland is a reclaimed tailings pond area previously classified as one of the most contaminated natural environments in the world [81,82]. The area received heavy metal(loid) inputs from a nearby stibnite processing plant from 1969 to 1974 [15,81,82]. After the separation in a floating cell, the residual tailings were deposited directly onsite without containment [15]. The impacted area was approximately 7.5 ha of wetland near the mouth of the Bellinger River. Significant rehabilitation and reclamation efforts have transformed this area as suitable for recreational amenity [81,82]. The Urunga soils have been reported to contain up to 2500 mg $kg^{-1}$ As and up to 22 000 mg $kg^{-1}$ Sb [15].

Since 1876, Au and Sb have been exploited in the Hillgrove Mineral Field, in the upper region of the Macleay River Catchment [17,83–85]. As a consequence of Au and Sb exploitation, more than 10 million tonnes of As and Sb-bearing wastes are estimated to have dissipated in the creek system that bisects the Hillgrove Mineral Field and have dispersed through the Macleay River system. Floodplain soils in the catchment contain greater than background concentrations of both metalloids [17,86]. In this study, we used the same floodplain soil as Doherty et al. [17] (FTFP in their study, termed MRC here, sampled at a different time) containing 15 ± 1 mg $kg^{-1}$ Sb and 21 ± 1 mg $kg^{-1}$ As reported in that study.

### 2.2. Microcosm experiment

Sieved (≤ 2 mm) soils were used for the microcosm experiments. The microcosm design was similar to Caplette et al. [71] and Caplette et al. [31], but the soils used in the present study were freeze-dried and not fresh. Each microcosm consisted of an autoclaved (121°C for 20 min), acid-washed 250 mL Erlenmeyer flask with a Drechsel bottle head. At one end of the Drechsel bottle's head, the in-flow air (atmospheric air) was passed through a 0.45 µm syringe filter and Sb trap (inlet trap) and the outflow air passed through an Sb trap (outlet trap) connected to a diffusor pump (600 mL $min^{-1}$) (Fig. 1a). All connections made with the Sb traps and microcosms were with Pt-cured silicone tubing. The soil was added to the Erlenmeyer flasks, 100 g for the MRC soil and 50 g for the Urunga soil, and incubated (HPP 260, Memmert GmbH + Co. KG, Buchenbach, Germany) at 30°C and 78% relative humidity, the approximate summer field conditions, in triplicate (n = 6, 3 replicate microcosms per soil), for 27 days (Fig. 1b).

Both microcosm experiments were waterlogged with approximately 200 mL of $N_2$-purged synthetic water. The composition of the synthetic water was 0.70 mM $Cl^-$, 0.24 mM $NO_3^-$, 4.1 mM $SO_4^{2-}$, 4.1 mM $Ca^{2+}$, 1.7 $Na^+$ mM, 0.97 $Mg^{2+}$ mM, and 0.19 $K^+$ mM. We used the same water composition as described in Caplette et al. [31] for consistency and because the field sites waters are are freshwater, but sometimes tidally inundated. A microcosm with synthetic water only (no soil, n = 1) was also used as an experimental blank. The microcosm results containing soils are not blank microcosm subtracted.

### 2.3. Soil, porewater, and volatile Sb sampling

Soil samples were collected before waterlogging and at the end of the microcosm experiment. Approximately 10 g of each soil was freeze-dried and stored for further analysis.

Porewaters were collected using a MOM Rhizon Sampler (PVC/PE tubing, Ø = 5 cm porous membrane, 0.15 µm pore-size, ecoTech Umwelt-Meßsysteme GmbH, Bonn, Germany), placed permanently within the soil mass. The Rhizon sampler was connected to a serum vacutainer (5 mL, BD, Allschwil, Switzerland) by a needle syringe at the time of porewater sampling. The microcosm porewater was collected at six-sampling times (1, 4, 6, 8, 11, 21, and 27 days). At each sampling time, pH and $E_h$ (ORP probe, Lazar Research Laboratories, L.A., USA) were measured using an airtight flow-through system. The $E_h$ measurements have been corrected to the standard hydrogen electrode.

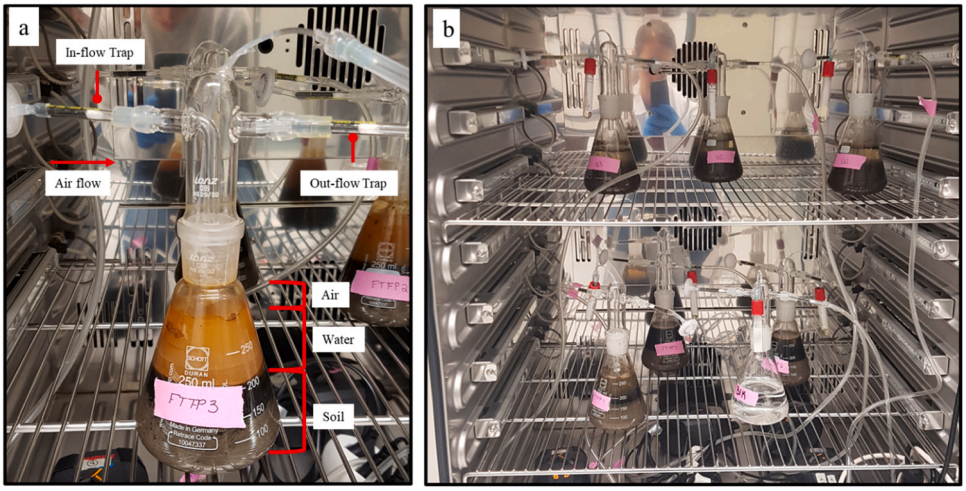


**Fig. 1.** a) the experimental design for the microcosm experiments and b) the entire experiment.

Aliquots for multi-element, Sb, ion chromatography (IC), dissolved organic carbon (DOC), and Sb speciation analyses were collected and stored until analysis at 4 °C. Samples were diluted for multi-element (1% $HNO_3$), Sb (1% $HNO_3$ + 0.5% HCl), DOC (ultra-pure water and acidified to pH < 2 with 10% HCl), IC (ultra-pure water), and Sb speciation (200 mM ammonium tartrate, pH 5). The microcosm surface waters were sampled on days 21 and 27, filtered (≤0.45 μm), and prepared for the same analyses as the porewaters.

The Sb traps were sampled at four time points (4, 11, 21, and 27 days) and stored at room temperature in the dark until microwave-assisted acid digestion. At each volatile Sb sampling time, the incubators were carefully re-watered, ensuring not to disturb the soil, to the starting mass with freshly prepared, $N_2$-purged, synthetic river water. The Sb traps were digested using an aqua regia closed vessel microwave digestion as described in S1.1 of the Supporting Information and Caplette et al. [71]. The Sb trap digests were stored at 4ºC in the dark until analysis.

All reported trap values were inlet trap subtracted to account for background contamination. The limit of detection (LOD) was calculated for each sampling time as 3.3 times the standard deviation (SD) of the inlet traps. When one of the three microcosms Sb traps was below the LOD, half of the LOD was used in calculations by convention. Samples below the LOD are reported as <LOD. The fluxes were calculated as the quotient of Sb trapped (ng) to the dry mass of soil and time.

### 2.4. Soil grain size, pH, and CN

For soil pH, 10 mL of 0.01 M $CaCl_2$ (1:5 m/v) was added to 2 g of the oven-dried soil. The soil was stirred, and the supernatant was measured after 2 h of equilibration. Grain size analysis was measured on the sieved, $H_2O_2$ pretreated soil fraction (Mastersizer 2000, Malvern PAnalytical Ltd., Malvern, United Kingdom).

For total soil carbon (C) and nitrogen (N), 10 to 40 mg of freeze-dried, ground soil was measured (Vario EL cube, Elementar Analysis system, Langenselbold, Germany) before and after loss on ignition (LOI, combusted at 550 °C for 2 h). The organic C ($C_{org}$) was calculated by subtracting the C concentrations after LOI. Standards of sulfanilic acid and glutamic acid, blanks, and sample triplicates were added for quality control.

### 2.5. Dissolved organic carbon and ion chromatography

An Elementar Vario TOC cube (Langenselbold, Germany) was used for DOC analysis porewaters and surface waters. Sample triplicates, blanks, and recovery checks were run every 20 samples. Porewaters and surface waters were also measured for dissolved anions ($SO_4^{2-}$, $NO_3^-$, $PO_4^{3-}$, $Cl^-$, $NO_2^-$) and cations ($Ca^{2+}$, $Na^+$, $K^+$, $NH_4^+$, and $Mg^{2+}$). An ion chromatography Dionex Aquion™ conductivity detector system (Thermo Fisher Scientific Inc., Waltham, USA) was used for the anion (buffer: 2.7 mM $Na_2CO_3$ and 0.3 mM $NaHCO_3$, column: Dionex™ IonPac™ AS12A (4×200 mm), suppressor: Dionex™ AERS™ 500) and cation (buffer: 20 mM MSA, column: Dionex™ IonPac™ CS12A (4×250 mm), suppressor: Dionex™ CSRS™ 300) analyses (injection volume: 100 μL, flow rate: 1 mL $min^{-1}$). Each measurement included sample triplicates, recovery checks, in-house reference materials, and blanks after every 20 samples. The QC recovery checks for anions analysis was 98.7 ± 3.5% and 99.3 ± 4.3% for cation analysis.

### 2.6. Volatile antimony traps

The Sb traps, composed of activated charcoal, were digested using a closed vessel aqua regia digestion outlined in S1.1 of the Supporting Information and Caplette et al. [71]. Inlet traps were used for background concentrations for the Sb traps, and all traps are inlet trap subtracted. Method blanks and blank traps were included in each digestion batch.

### 2.7. Soil digestions

Microcosm soils were digested for Sb and multi-elements according to the protocol outlined in S1.2 and S1.3 of the Supporting Information. Sample triplicates, method blanks, and certified reference materials (CRMs, (San Joaquin soil NIST-2709a and Montana II soil 2711a, Sigma Aldrich Buchs, Switzerland) were included in the digestions and measurements. The CRM recoveries are reported in Table S1 of the Supporting Information.

### 2.8. Elemental analysis

An Agilent 7700x series ICP-MS (Agilent Technologies, Waldbronn, Germany) was used for Sb and multi-elements analysis. Refer to Caplette et al. [71] for further instrument and analysis details. The LOD for Sb in the soil (< 0.25 mg $kg^{-1}$) and porewater (< 0.008 μg $L^{-1}$) was calculated from method blanks.

### 2.9. Antimony speciation

High performance liquid chromatography (HPLC) post-column UV-pre-reduction hydride generation (HG) atomic fluorescence spectroscopy (AFS) (PSA 10.820 modular interface equipped to an Excalibur AFS, PS Analytical, Kent, United Kingdom)) was used for Sb speciation analysis. Separation of $Sb^V$, TMSb, and $Sb^{III}$ was accomplished using a Hamilton PRP X-100 anion exchange column (10 μm, 150×4.6 mm (PEEK) Reno, NV., isocratic elution, flow rate: 1.2 mL $min^{-1}$), a 250 μL sample loop, with 200 mM ammonium tartrate (99.5%, Sigma Aldrich St Louis, MO, USA) in 4% MeOH (99.9%, Merck Millipore Inc. Burlington, USA) at pH 5. Samples were pre-reduced online with 0.5% (m/v) L-cysteine (99%, Merck Millipore Inc. Burlington, USA) in 30% (v/v) HCl. Before HG, the samples were oxidized using UV light and heat (120ºC). Once introduced into the gas-liquid separator, a solution of 1% $NaBH_4$

**Table 1**
Table comparing the amount of volatile Sb produced in shooting range (SR), Chinese rice paddy soils (CRP), alluvial soil (AS), Urunga (U) and Macleay River Catchment (MRC) soils from this study.

| Sample | Soil pH | Texture | $C_{org}$ | C/N | Soil Sb | Cumulative Volatile Sb | Volatile Sb after 28 Days | Sb Volatilized from Soil | Reference |
|---|---|---|---|---|---|---|---|---|---|
| | | | % | | mg $kg^{-1}$ | ng $kg_{soil}^{-1}$ | ng $kg_{soil}^{-1}$ | % | |
| CRP | 6.4 - 6.7 | silt Loam | 2.5 - 4.9 | 11.7 – 17.1 | 116 - 431.5 | 0 - 415.5 | 0 - 286 | 0.00002 - 0.000085 | Caplette et al. [31] |
| SR | 6.8 | sandy Loam | 2.7 | 21.2 | 75 ± 6.2 | 0 - 1969 | 0 - 400 | 0.0004 - 0.002 | Caplette et al. [71] |
| AS | 5.8 - 6.9 | NA | 3.5 | 17.5 | 1.3 | 33346 | 340 | 2.8 | Meyer et al.[78] |
| U | 4.14 | sandy Loam | 23.9 | 25.5 | 1251.7 ± 24.9 | 409 - 835 | 410 - 835 | 0.00003 - 0.00007 | this study |
| MRC | 3.58 | silt Loam | 9.3 | 13.2 | 15.0 ± 0.1 | 54 - 337 | 55 - 337 | 0.0004 - 0.002 | this study |

(> 98%, Sigma-Aldrich Inc., St. Louis, USA) in 0.1 M NaOH (Carl Roth, 99%, Karlsruhe, Germany) was used to reduce inorganic Sb and TMSb to their hydride and/or volatile forms. A boosted discharge hollow cathode superlamp ($\lambda = 217.6$ nm, Gesellschaft fuer Analysentechnik HLS, Salzwedel, Germany) was used as the excitation source.

The LOD for our analysis was 2.5 μg $L^{-1}$ for TMSb (250 μg $kg^{-1}$ in the soil) and was determined by injecting six blanks and standards around three times the baseline value and multiplying the average by 3 times the standard deviation. The LOD of $Sb^{V}$ was 0.2 μg $L^{-1}$ and 0.1 μg $L^{-1}$ for $Sb^{III}$ calculated from the calibration curve.

For porewater Sb speciation analysis, the column and Sb speciation spike recoveries are reported in Table S2 of the Supporting Information as the ratio of the sum of species in the speciation analysis to the total Sb concentration in the porewaters. Spike recovery was 72 to 108% and 109.2% for TMSb in porewater and surface water, respectively. Generally, at the beginning of the microcosm experiment, column recoveries were 86.3 to 99.8%. The porewaters from later sampling days corresponded to a decrease in column recoveries to 36.6% (Supporting Information, Tables S2 and S3). The poor column recoveries in our analysis may indicate that other species which retain on the column Sb species were formed in the waters during the incubation.

For soil Sb speciation, the column recoveries are reported in Table S4 of the Supporting Information. The QC recovery checks for $Sb^{V}$ were 96.1 to 99.4%, 97.4 to 105.1% for TMSb, and 96.6% for $Sb^{III}$. Spike recovery for TMSb was 88.9 ± 8.1% (Supporting Information, Table S5). Speciation conversions were observed for the soil spiked with inorganic Sb species (Supporting Information, Table S4). Extraction efficiencies were calculated as a percentage of the sum of extracted species (mass basis) during speciation analysis to the total Sb concentration in the soil.

#### 2.9.1. Trimethylantimony extraction from soils

The method outlined by Grob et al. [26] was used to extract TMSb from the soil. This method is not quantitative for inorganic Sb speciation because $Sb^{III}$ and $Sb^{V}$ species can be oxidized and reduced, respectively, during the extraction process [26,87], but it is suitable for TMSb extraction from soils.

Briefly, 100 mg of freeze-dried soil from each microcosm was weighed into borosilicate glass vials and a 10 mL solution of 200 mM oxalic acid (99%, Merck Millipore Inc., Burlington, MA, USA) and 100 mM ascorbic acid (99.7%, Merck Millipore Inc., Burlington, MA, USA) was added to the soil. The soil and solution mixture were well mixed and then ultrasonicated for 30 min in the dark. After ultrasonication, it was centrifuged for 5 min at 3500 rpm. The supernatant was filtered ≤ 0.2 μm, stored at 4°C, and diluted in the buffer (150 mM ammonium tartrate, pH 5) for analysis. Quality control during the extraction process included method blanks and soil spikes of $Sb^{V}$ (150 mg $kg^{-1}$), $Sb^{III}$ (150 mg $kg^{-1}$), and TMSb (5 mg $kg^{-1}$) on uncontaminated soil (3.7 mg $kg^{-1}$ Sb).

#### 2.9.2. Conversion of antimony-species standards

When the $Sb^{V}$ standard was prepared in the ammonium tartrate buffer, there was an $Sb^{III}$ peak present in the chromatogram, indicating reduction in buffer (Supporting Information, Fig. S1). The $Sb^{V}$ standard was subsequently prepared separately in ultra-pure water to prevent this.

Due to potential conversion in the buffer of $Sb^{V}$ to $Sb^{III}$, individual inorganic Sb species quantification is likely not accurate and instead is represented as the total inorganic Sb. Porewater samples from the MRC microcosms had severe matrix effects and presented complications with chromatographic measurements. Due to the lower Sb concentration in the MRC samples, they could not be further diluted. The QC recoveries were 96.5 ± 8.4% for $Sb^{V}$, 97.0 ± 3.8% for TMSb, and 97.0 ± 8.2% for $Sb^{III}$ from QC standards from the respective species. Porewater standard spike recoveries for TMSb were 72 to 108% and for $Sb^{III}$ 80 to 120%.

### 2.10. Statistical treatment of data

Paired and unpaired t-tests ($p < 0.05$, Microsoft Excel 2021) were used to determine statistical differences. Pearson's r was used to assess correlations between data; statistically significant correlations were defined as $p < 0.05$.

## 3. Results

The chemical and physical parameters for the soils are presented in Table S1 of the Supporting Information. The Urunga soil was an acidic (pH of 4.14) sandy Loam with $C_{org}$ of 23.9%, a C/N of 25.5 and 1251.7 ± 24.9 mg $kg^{-1}$ Sb, 4.4 ± 0.2 g $kg^{-1}$ Fe, and 39.7 ± 1.7 mg $kg^{-1}$ Mn. Compared to the Urunga soil, the MRC soil had a finer texture (silt Loam), is more acidic (pH of 3.58), contains less $C_{org}$ (9.3%), has a lower C/N of (13.2) (Table 1), and less soil Sb (15.0 ± 0.1 mg $kg^{-1}$). The MRC soil had greater concentrations of Fe and Mn than the Urunga soil (Table S1).

### 3.1. Development of porewater pH and $E_h$, and release of Fe, Mn, and $SO_4^{2-}$

The results for porewater pH are shown in Fig. 2a-b. In both soils, the porewater pH increased temporally, but the MRC (3.5 to 6.8) microcosms pH increased more than in the Urunga soil (4.5 to 5.5) throughout the experiment.

The $E_h$ was measured in the porewaters throughout the experiment except for two measurements (days 6 and 8) due to sampling complications (Supporting Information, Fig. S2). The initial $E_h$ for the Urunga soil was + 300 to + 450 mV and the MRC soil was + 500 mV (Supporting Information Fig. S2). While the $E_h$ for the MRC soil continued to decrease (+47.7 ± 3.5 mV) until the end of the microcosm experiment, the Urunga soil plateaued around 11 days after waterlogging (+273.3 ± 12.4 mV) (Supporting Information, Fig. S2).

The Fe sampled from the blank microcosm was below the instrument LOD and showed 0.1 ± 0.07 μg $L^{-1}$ Mn, much less than the measured concentrations in the soil microcosms indicating minimal background Fe and Mn in our microcosm experiments. The porewater $SO_4^{2-}$ concentrations in the blank microcosm were relatively consistent throughout the experiment and were similar ($p > 0.05$) to the concentration in the synthetic river water.

On the 4th day of waterlogging, a spike in Fe concentration was observed in the porewaters of both soils (Urunga: 44.8 to 47.7 mg $L^{-1}$, MRC: 1505.6 to 1697.8 mg $L^{-1}$, Fig. 2c-h). Immediately with waterlogging, high Mn (Urunga: 1.0 to 1.2 mg $L^{-1}$, MRC: 27.5 to 31.4 mg $L^{-1}$) and $SO_4^{2-}$ (day 4, Urunga: 481.9 to 507.88 mg $L^{-1}$, MRC: 4176.5 to 4527.3 mg $L^{-1}$) was observed in both soils (Fig. 2e-h). On the last day (day 27), soluble Fe, Mn, and $SO_4^{2-}$ decreased in the porewaters (Fig. 2c-h).

### 3.2. Dissolved organic carbon

The Urunga soils had high DOC in the porewaters (369.7 to 581.5 mg $L^{-1}$) at the beginning of the experiment which decreased after 11 days of waterlogging (Fig. 3a). The DOC in these porewaters was negatively correlated with porewater pH ($r = -0.7$, $p < 0.05$) and positively with $SO_4^{2-}$ and $E_h$ ($r = 0.72$ to 0.76, $p < 0.05$) (Fig. S3).

After 4 days of waterlogging, a decrease in DOC was detected in the porewaters of the MRC soils (154 to 211 mg $L^{-1}$). An increase was observed afterward until day 11 and then generally stabilized until the end of the experiment with a slight decrease in concentration on day 22 (731 ± 77 mg $L^{-1}$) (Fig. 3b). Here, the DOC was correlated with porewater pH and As ($r = 0.79$, $p < 0.05$), and negatively with $SO_4^{2-}$, $E_h$, Mn, and Ni ($r = -0.64$ to $-0.79$, $p < 0.05$) (Fig. S4).

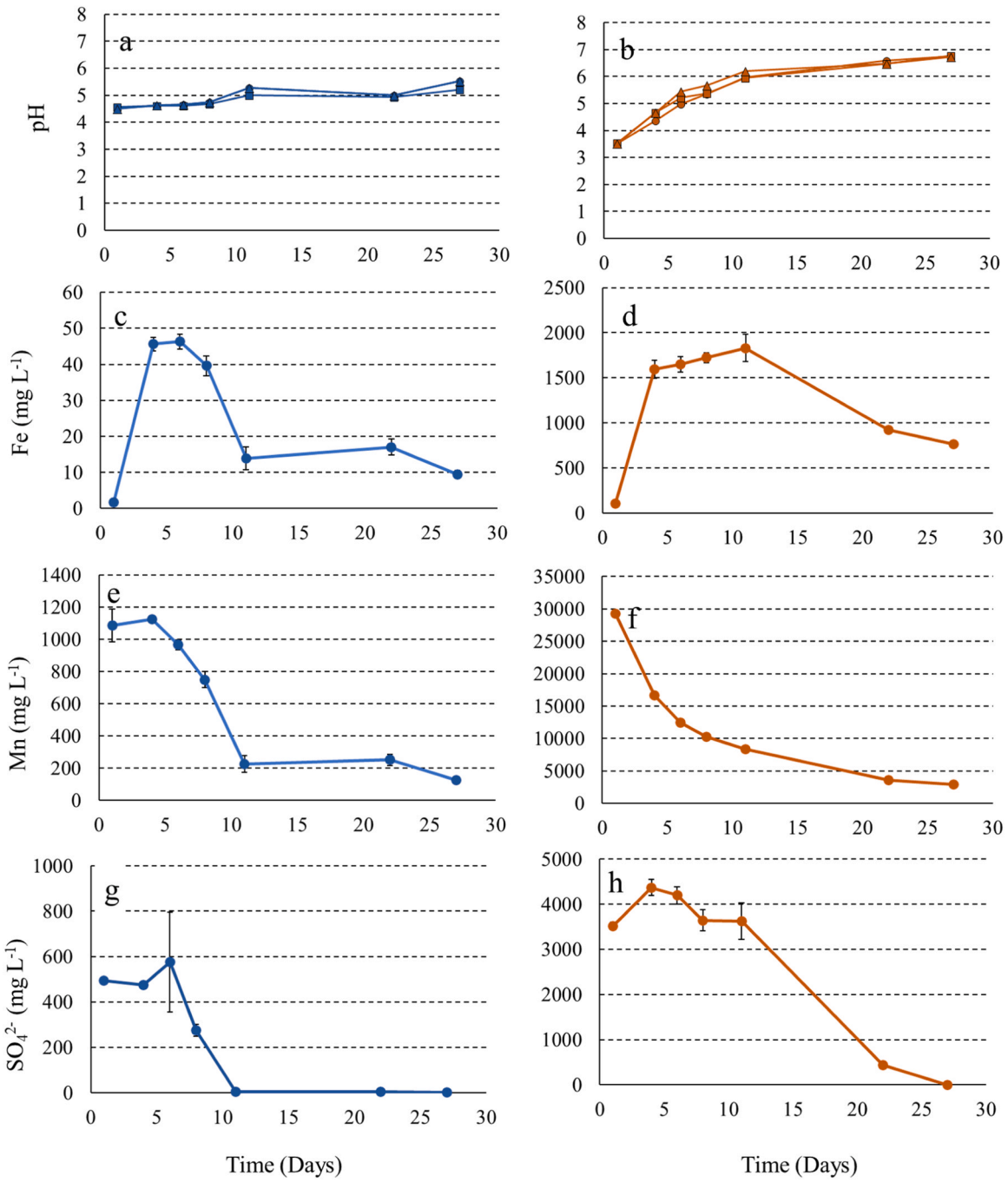


**Fig. 2.** Temporal results for Urunga (blue) and MRC (orange) for porewater a-b) pH, c-d) Fe, e-f) Mn, and g-h) $SO_4^{2-}$. Symbols represent microcosm replicates; circle (microcosm 1), square (microcosm 2), and triangle (microcosm 3) for the pH measurements.

### 3.3. Porewater antimony: release and speciation

#### 3.3.1. Total antimony release into the porewaters

The release of Sb in the Urunga soil was sudden and high on the first day of waterlogging (increasing from 3240.0 ± 172.7 μg $L^{-1}$), but porewater concentration decreased and stabilized by day 8 (611.9 ± 14.7 μg $L^{-1}$) (Fig. 3c). Sb was released at a slower rate in the MRC soil and increased to a maximum on the 11th day of waterlogging (34.9 ± 4.2 μg $L^{-1}$) and then decreased (Fig. 3d).

#### 3.3.2. Porewater antimony speciation

Despite the lower column recoveries for the porewater, the sum of the inorganic species in the Urunga porewaters behaved similarly to the total Sb in the porewaters. After 6 days of waterlogging, we observed a species in the porewater that did not align with any of the Sb standards available with a retention time of 4.2 min (Fig. 4 and Supporting Information, Fig. S6). The development of an unknown species increased in the porewaters until the 11th day of the waterlogging and then generally began to decrease in most microcosms except for the third replicate (Fig. 4).

Porewater samples were spiked (two times the peak area) with a TMSb and $Sb^{III}$ standard for species identification. Spiked samples with TMSb and $Sb^{III}$ did not align with this peak and, therefore, it is unlikely to be TMSb (Supporting Information, Fig. S6). It may be inferred that as the species is HG-reactive it could potentially be another organic-Sb species but due to a lack of commercially available Sb standards we

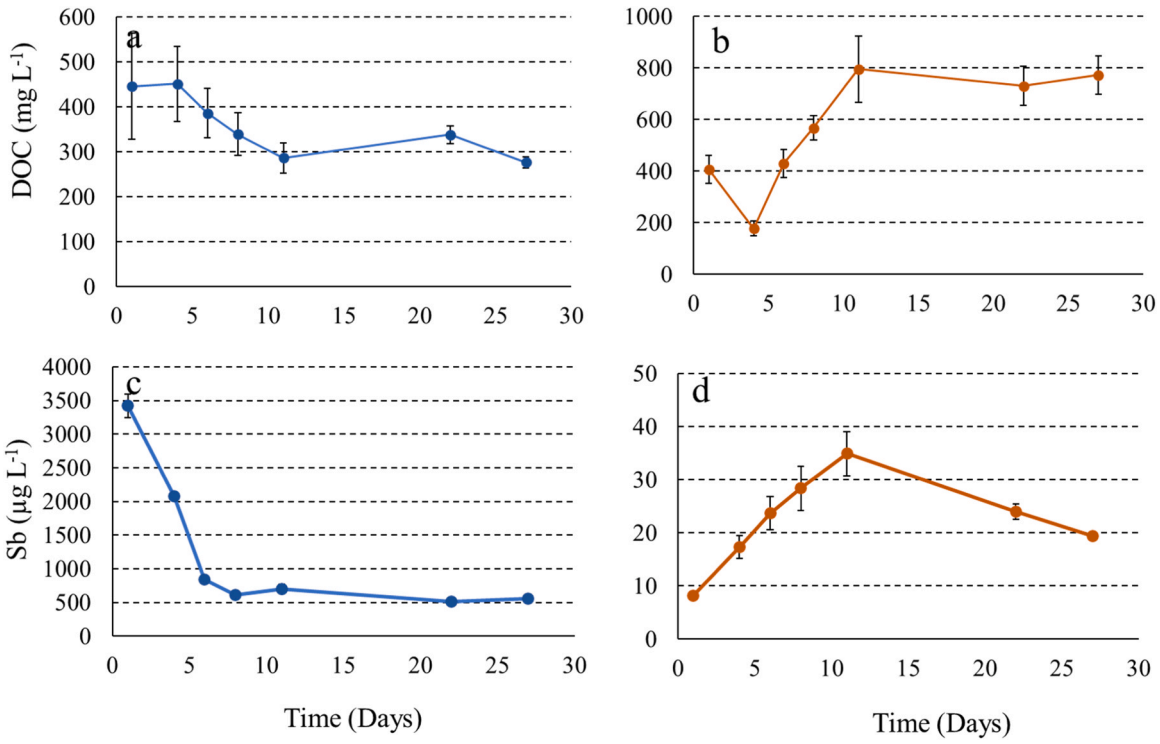


**Fig. 3.** Temporal results in the porewaters for Urunga (blue) and MRC (orange) microcosms for a-b) DOC and c-d) Sb.

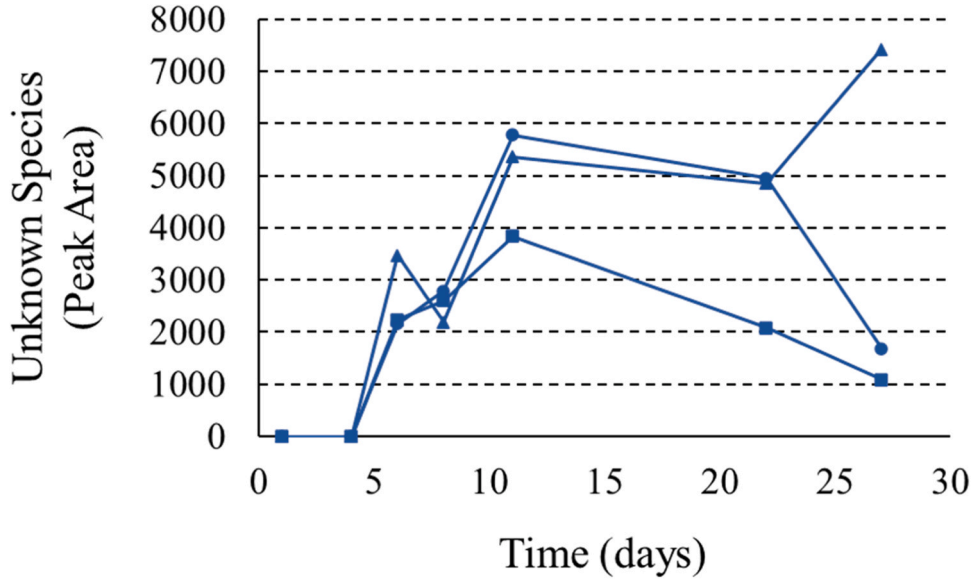


**Fig. 4.** Temporal results of peak area of unknown Sb species in the porewater of the Urunga microcosms. Symbols represent microcosm replicates; circle (microcosm 1), square (microcosm 2), and triangle (microcosm 3).

were unable to further identify this species. Furthermore, since Sb species have species-specific sensitivities using AFS this species could not be quantified.

Speciation samples for the surface waters were collected on the last two sampling days. In the surface waters there was an observed retention time shift for all Sb species by at least 20 s earlier. The observed shift for the TMSb standard was from 5.3 min in the porewaters to ~4.5 min (Supporting Information, Fig. S6). Spiked surface water samples showed overlap of peaks and poor separation of the spiked TMSb standard and unknown species. Taking into account the retention time shift for TMSb (4.5 min), and the presence of the unknown species (at 4.2 min) in the porewaters with a similar retention time, spiking was not viable for differentiation of the species. This species may be TMSb, but also may be the TMSb standard eluting at a similar time as the unknown species due to matrix effects in the surface waters. The sample could not be further diluted due to the already low amount of the unknown species. The peak area for the species was constant throughout the different sampling times ($p > 0.05$).

### 3.4. Soil antimony speciation

The soils before and after the microcosm experiment were extracted

for TMSb. The extraction efficiency, column recoveries, and soil spike recoveries are reported in Tables S4 and S5 of the Supporting Information.

There was an observed shift in retention time for all Sb species in the soil extractions. This may be due to matrix effects in the soil extracts. Soils extraction before the microcosm experiment contained inorganic Sb and a species with a retention time of ~ 4 min (Supporting Information, Fig. S7). Soil extracts were spiked with TMSb and $Sb^{III}$ to approximately 2 times the peak area (Fig. S7 in the Supporting Information) for species identification.

Although there was an apparent peak overlap/poor seperation between the spiked TMSb and the species in the un-spiked samples, there was ~30 s between the TMSb and unknown species retention time, therefore species identification remained unclear (Supporting Information, S8.2.2) due to the shift in retention time due to a potential matrix effect in the extracts. The unknown species in the porewater and soil extracts have a similar retention time which may cause the TMSb spike to elute earlier (Fig. S7). Here, a more conservative approach is taken, and the species is referred herein as the unknown species due to the 30 sec difference in retention time although there is poor species separation. The unknown species' peak area before and after the microcosm experiment was variable. The first and second replicates were similar to the pre-waterlogging peak area, but the third replicate was less (3.2 times) than the pre-waterlogging peak area.

### 3.5. Antimony volatilization from microcosms

In both soils, volatile Sb was detected on the 11th day of waterlogging (Fig. 5 and Table S6 in the Supporting Information). With time, more volatile Sb was produced (Fig. 5). The Urunga soil stopped producing volatile Sb on the last day of incubation (Fig. 5a). The Urunga soils produced cumulatively more volatile Sb, 655.6 ± 220.7 ng $kg_{soil}^{-1}$, than the MRC soils, 181.8 ± 143.1 ng $kg_{soil}^{-1}$ ($p < 0.05$) (Table S6). On the last day, volatile Sb was <LOD for the Urunga soils. The maximum volatile Sb was produced on day 22 after waterlogging in the Urunga soils (353.9 to 723.1 ng $kg_{soil}^{-1}$) and on the last day for the MRC soils (25.8 to 268.4 ng $kg_{soil}^{-1}$). The volatilization of Sb from the Urunga soil stopped by the last day of the experiments while volatile Sb was detected in the MRC soil (Fig. 5, Table S6).

## 4. Discussion

### 4.1. Environmental relevance: soil quality and impact of waterlogging on water quality

The Sb concentration in the Urunga soil was approximately 40 times higher than the European Union (37 mg $kg^{-1}$) threshold values for agricultural soils [88]. The large Sb pool in the soil indicates a risk for Sb remobilization with waterlogging (e.g., potential release from the solid phase). Our total Sb results were lower than those previously reported for Sb for soil collected from this site by Ngo et al. [82] and Warnken et al. [15], but are consistent with the findings of Bennett et al. [13]. In an organic-rich sediment from the same location, XAS analysis showed that Sb was mostly present as $Sb^{III}$-phases and 44% of the $Sb^{III}$-phase was as a highly disordered Sb phase complexed with reduced sulfur either with thiol-groups on organic matter or an amorphous $SbS_3$ phase [13].

The Sb concentration (15.0 ± 0.1 mg $kg^{-1}$) in the MRC soil was lower than the European Unions threshold values for agricultural soils and was consistent with soil Sb concentrations reported in Doherty et al. [85] (Table S1 in the Supporting Information). An XAS analysis on soil sampled from the same location, but at a different time, showed Sb solid-phase speciation was dominated by $Sb^{V}$ (82.6%) [89]. Sequential extractions showed that Sb in the soil was typically associated with the reducible fractions [89], which agrees with the Sb release patterns in our porewaters (Fig. 3d, discussed below). As the MRC soil is an agricultural floodplain soil and frequently influenced by tidal inundation, Sb may be released when solid phases (e.g., Fe-(oxyhydr)oxides) are reductively dissolved [20,21,35]. Frequent redox cycling influenced by wetting and drying cycles in this region may further enhance Sb sequestration by incorporating Sb into more crystalline phases [89,90].

In our experiment, the maximum proportion of Sb released from the soils was similar ($p > 0.05$) in the Urunga (0.27%, 1st day after waterlogging) and MRC (0.23%, 11 days after waterlogging). Both soil porewaters exceeded the 9 μg $L^{-1}$ Sb guideline value for Australian freshwaters [91] (no value has been established for marine waters) immediately (Urunga) or after 4 days (MRC) of waterlogging and were consistently higher than this threshold value for the experiment length. In the Urunga soil, even when Sb in the porewaters decreased to its minimum value, the concentration was approximately 55 times higher than the freshwater regulatory limit. The Urunga surface water Sb concentrations (516.2 to 657.0 μg $L^{-1}$, $p > 0.05$) were similar to the porewaters, but this was not the case in MRC, in which concentrations were lower than porewaters (4.8 to 9.5 μg $L^{-1}$, $p < 0.05$). This observation indicates that diffusion from the porewaters to surface water does not occur for the MRC soil to the same extent as observed in the Urunga soil. Our results indicate, because the Urunga soil is permanently waterlogged, and the MRC soil is frequently waterlogged, that Sb may be released for both soil types and may impact surface water quality.

### 4.2. Release of Sb under waterlogged conditions

#### 4.2.1. Organic-rich soil

The release of Sb into the porewaters of the organic-rich soil was immediate with waterlogging with up to 3420 μg $L^{-1}$ Sb released into the porewaters (Fig. 3c). A similar initial rapid-release pattern of Sb with waterlogging for the Urunga soils has been also reported in Chinese rice paddy soils [31], Swiss shooting range soils [26,27,92] and mine dump soils [93]. This initial, rapid release of Sb into the porewaters may be

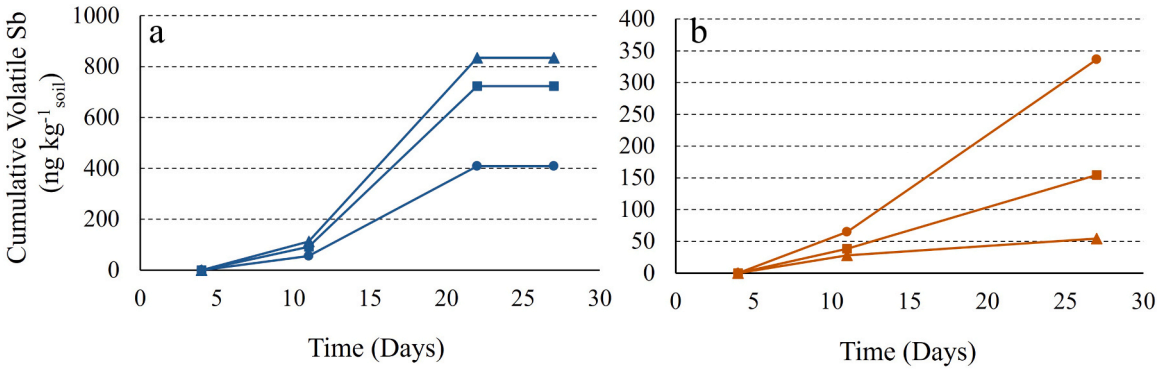


**Fig. 5.** Cumulative volatile Sb produced (ng $kg_{soil}^{-1}$) for the duration of the microcosm experiment for a) Urunga and b) MRC microcosms. Symbols represent microcosm replicates; circle (microcosm 1), square (microcosm 2), and triangle (microcosm 3).

due to the desorption of weakly bound Sb on the solid-phase and solubilization of high-solubility salts in the soil [26,31].

#### 4.2.2. Fe-rich floodplain soil

Under waterlogged conditions, between days 1 to 11, porewater Sb release in the MRC soil increased (Fig. 3d). An increase in porewater Fe (from 106 ± 10 to 1595 ± 97 mg $L^{-1}$) on day 4 indicates the onset of Fe-reduction (Fig. 2d). There was general increase in porewater Fe, DOC, and Sb concentration until day 11 after waterlogging (Figs. 2b and d and 3d). This suggests that the release of Sb is associated with the reductive dissolution of Fe-(oxyhydr)oxides in the soil and is further supported by the association of Sb with the reducible fractions (e.g., Fe-phases) in the same soils (but sampled at a different time) [89]. In the MRC soil, porewater Sb was also correlated strongly with porewater pH, Fe, and DOC ($r = 0.57$ to 0.78, $p < 0.05$) (Fig. S4). In soils, Sb forms innersphere complexes to Fe-oxyhydroxides and can also be structurally incorporated into these phases [27,35,89].

### 4.3. Immobilization of Sb under waterlogged conditions

#### 4.3.1. Organic-rich soil

Porewater Sb rapidly decreased from 3420 μg $L^{-1}$ on day 1 to 612 μg $L^{-1}$ by day 8 (Fig. 3c). The decreasing trends of Sb in the porewaters was similar to the observed trends for Mn, $E_h$, DOC, and $SO_4^{2-}$ (Figs. 2e, g, 3a, c and S2) but was dissimilar to porewater Fe (Fig. 2c). The high concentrations of Mn and Fe in the porewaters suggest the onset of Mn and Fe reduction on the 1st and 4th day after waterlogging, respectively (Fig. 2c and e). Decreasing concentrations of porewater $SO_4^{2-}$ from 495 mg $L^{-1}$ on day 1 to below DL on day 11 indicate $SO_4^{2-}$ reduction and potential formation of reduced sulfur species. Sulfate-reduction was indicated by the loss of $SO_4^{2-}$ in the porewaters and declining $SO_4^{2-}$:$Cl^-$ molar ratios (Supporting Information, Fig. S5), where a decrease in the ratio indicates $SO_4^{2-}$ reduction [31,94]. In our experiments the redox potential did not reach the theoretical redox potential for $SO_4^{2-}$ reduction (−100 mV) [16,24,95], possibly because our measurements were averaged readings of $E_h$ in the microcosm. A lower redox may exist in localized pore spaces consistent with the observed $SO_4^{2-}$ reduction. Similar results have been reported in the porewaters of Chinese rice paddy microcosms [31], floodplain soils [28,94] and shooting range soils [26] when using a similar method for measuring $E_h$. Weber et al. [28] showed in a waterlogged floodplain soil that $SO_4^{2-}$ was consumed by days 4 to 10, before Fe-reduction; simultaneously with Mn-reduction.

In soils, Fe-(oxyhydr)oxides commonly act as Sb sinks in aerobic and anoxic soils [33,35,96]. If Sb was pre-dominantly associated with Fe-(oxyhydr)oxides in the Urunga soil, Sb release should mirror (or correlate with) the release of Fe in the porewaters. Our results suggest that Sb is more closely associated with $E_h$, pH, DOC, $SO_4^{2-}$, and Mn ($r = 0.65$ to 0.97, $p < 0.05$) but not Fe ($r = -0.24$, $p > 0.05$, $n = 21$) (Fig. S3). An organic-soil collected from the same wetland showed that Fe-phases were not major sinks of Sb, and Sb did not re-bind to Fe-(oxyhydr)oxides [15].

Correlations between Sb and DOC ($r = 0.65$, $p < 0.05$, $n = 12$), $SO_4^{2-}$ ($r = 0.66$, $p < 0.05$, $n = 12$), and Mn ($r = 0.7$, $p < 0.05$, $n = 12$) indicate that multiple mechanisms may be occurring in the Urunga porewaters simultaneously. For example, DOC may be used as an electron donor for microbial reduction, and sulfate reduction can produce reduced sulfur species [95,97] or compete with Sb for binding sites [26,98]. The reduced sulfur species may be incorporated into the natural organic matter as thiol groups, which can form covalent bonds with $Sb^{III}$ [38,39] but can also facilitate Mn reduction [99], or promote the production of authigenic Fe-sulfides and Sb sulfides [3,13,32]. Both mechanisms could decrease Sb in the porewaters. Furthermore, DOC can complex and co-precipitate with metal oxides such as Mn-oxyhydroxides [47,100,101]. The recrystallization of birnessite (MnOOH) to MnOOH-polymorphs induced by $Mn^{II}$ has been shown to reduce $Sb^V$ mobility [102]. Studies on soils from the same wetland showed that Sb was decoupled from the Fe cycle and associated with sulfur, either as a discrete sulfide ($SbS_3$) or with thiol groups on organic matter [3,13,15].

#### 4.3.2. Sb immobilization in the Fe-rich floodplain soils

After the 11th day of waterlogging, porewater Fe, $SO_4^{2-}$, and Sb concentrations rapidly decline (Figs. 2d and h, and 3d). The rapid reduction of porewater $SO_4^{2-}$ concentrations from 3622 mg $L^{-1}$ on day 11 to below DL on day 22 suggest that $SO_4^{2-}$ reduction may be occurring in MRC soil (Fig. 2h). Sulfate-reduction was indicated by the loss of $SO_4^{2-}$ in the porewaters and declining $SO_4^{2-}$:$Cl^-$ molar ratios (Supporting Information, Fig. S5), where a decrease in the ratio indicates $SO_4^{2-}$ reduction [31,94]. Sulfate reduction produces reduced sulfur species which can subsequently precipitate as sulfides under anoxic, waterlogged conditions (e.g., iron sulfides or metal sulfides) [97,103].

Figs. 2d, h, and 3d show a decrease in the concentrations of Fe, $SO_4^{2-}$, and Sb in the MRC porewaters. This observed decrease in Fe and Sb in the porewaters was strongly correlated with $SO_4^{2-}$ ($r = 0.96$, $p < 0.05$, $n = 9$ for Fe and $r = 0.94$, $p < 0.05$, $n = 9$ for Sb) suggesting that Sb may be co-precipitating with Fe-sulfide phases (e.g., $SbS_3$, mackinawite, amorphous FeS, and/or pyrite). This suggests that under reducing conditions, Fe is initially released by microbial Fe-reduction but quickly (within days) immobilized with the formation of Fe-sulfide phases (e.g., mackinawite (FeS), pyrite ($FeS_2$), and amorphous $FeS_x$) (Fig. 2d) [103,104]. Hockmann et al. [32] showed that during Fe-oxide sulfidization, the reductive dissolution of ferrihydrite released $Sb^V$. After 1 to 7 days, $Sb^V$ was immobilized by the sorption to secondary Fe-oxides and authigenic Fe-sulfides (mackinawite and pyrite) at pH 6 [32]. Our porewater pH during the Sb loss phase was between 6 and 6.8 (Fig. 2b). In a tidally influenced acidic wetland soil, Fe-sulfides precipitated with reflooding of the wetland and meta-stable greigite ($Fe_3S_4$) and pyrite were detected in the sediment [104]. Reductive dissolution of $Fe^{III}$-phases in sulfidic, floodplain sediments from the Clarence, Richmond, and Tweed Rivers, Australia produced an abundance of $Fe^{II}$ and reduced sulfur in the porewaters [97]. Paralleled with an increase in porewater pH (>5.5) from microbial degradation of organic matter, disordered mackinawite and siderite ($FeCO_3$) were precipitated [97]. Our data indicate that with the onset of reductive dissolution of $Fe^{III}$-phases in the soil a similar mechanism may be occurring in our microcosm. Secondary Fe-sulfides may be precipitating with the onset of sulfate reduction and subsequent formation of reduced sulfur species, and co-precipitating/sorbing Sb, in turn, immobilizing Sb.

Both the Urunga and MRC samples are wetland soils, but with very different soil Sb concentrations. The fate of Sb in the two soils was also different, either linked to the Mn, C, and S cycles (Urunga) or the Fe and S cycles (MRC); and this difference accounted for variable risks with waterlogging of the two soil types. Nevertheless, both soils released environmentally relevant concentrations of Sb with waterlogging, indicative of potential risk to the surrounding environment.

### 4.4. Transformation of Sb in waters of Urunga soil

The unknown species in the Urunga porewaters correlated with $E_h$ ($r = -0.79$, $p < 0.05$, $n = 9$) which indicates this species was released or formed under more reducing conditions. In effect, waterlogging may result in enhancing Sb mobility, at least temporarily.

Due to a lack of available Sb standards we could not successfully identify the unknown species, but reports of an unknown species at a similar retention time, using the same buffer as this study, was identified in soil extracts [26,105]. Low column recoveries in the porewater samples indicates that there may be retained and unidentified species therein. This is supported by the lack of significant correlation between the unknown species and retained Sb ($r = 0.02$ to 0.72, $p > 0.05$). Although further investigation into species identification should be done on the soil extracts. These results highlight the importance of further investigation into Sb speciation, the need for adequate standards, and

the current limitations on our understanding of Sb transformations.

### 4.5. Antimony volatilization in soils: relevance and drivers

A comparison between the instantaneous volatile Sb and cumulative volatile Sb fluxes with porewater (Table 2) and surface water Sb did not yield any significant correlations. Volatile Sb may be produced in the surface waters, similar to Chinese rice paddy soils [31], but it was not possible to draw this conclusion due to the small data set.

If volatile Sb was produced in the porewaters, like volatile As [76], 0.003 to 0.06% of the Urunga porewater Sb was volatilized while the MRC volatilized 0.03 to 1.3% of the porewater Sb. If Sb was volatilized from the surface waters, as suggested in our previous work [31], 0.04 to 0.09% of the porewater Sb in the Urunga microcosms was volatilized and 0.4 to 7.4% from the MRC microcosms. Although in this study, the Urunga soil produced more volatile Sb throughout the duration of the experiment, volatilization from the soil Sb pool was 18.2 times less ($7\times10^{-5}$ %) than the MRC soil (0.002%) (Table 1). Also, different volatilization behavior was observed between the soil types (Fig. 5). In the case of the Urunga soil, Sb was volatilized temporarily in the microcosms and could indicate that Sb volatilization was produced intermittently with changes in redox potential, but longer experiments would be needed to confirm this.

When the volatile Sb produced in this study was compared at similar experimental lengths in the aforementioned studies, the volatile Sb produced from the Urunga soils was higher than all waterlogged treatments without manure in the shooting range soils [71] and Chinese rice-paddy soils ($p < 0.05$) [31]. The manured treatments produced comparable amounts of volatile Sb as the Urunga microcosms ($p > 0.05$) likely due to microbial stimulation [106]. The soils in this study were not amended but contained naturally high amounts of organic matter (Table 1) and C/N ratios that are favorable for microbial activity (13 and 25). Additionally, the DOC in the porewaters of the MRC soil was higher than the Urunga soil and may indicate more available C to fuel volatilization but future works should investigate this. These properties may explain the similar amounts of volatile Sb produced when compared with those found in the amended soils.

The first appearance of volatile Sb in the microcosms corresponded to a porewater pH of 5 (Urunga) and 6 (MRC). For volatile As species (trimethylarsine) production and As methylation, the optimum pH range is 5 to 6 [21,107–109]. Currently, there is limited knowledge about Sb volatilization drivers in soils. If the pathway for volatilization is similar As volatilization [110,111], it may be that favorable volatilization conditions for As (e.g., pH) are also favorable for Sb volatilization. Physical soil parameters are known to influence As volatilization and methylation. For example, temperature [112,113], soil texture [113,114], moisture content [108,115], nutrients [31,71,75,77,106,116], and pH [107,108,117] and may also impact Sb volatilization. Based on several studies, microorganisms may volatilize Sb once conditions are favorable [14,69,78,108,118,119].

Although in this work we did not find any direct links between the soil, porewaters, or surface waters with Sb volatilization (Table 2), we did detect volatile Sb in two different soil types. Interestingly, higher soluble Sb and a larger Sb pool do not volatilize Sb more efficiently, since the MRC soils volatilized up at 18 times more Sb from the soil pool than from the Urunga soil. Soluble metal(loid)s are assumed to be bioavailable and this indicated that higher bioavailability of Sb does not directly lead to a higher volatilization rate. In microflora from sewage digesters, Michalke et al. [53] showed that higher concentrations of Sb substrates did not yield higher production of volatile Sb. This work is in agreement with the findings by Caplette et al. [31,71] and Meyer et al. [78], where the authors showed that soils with higher Sb concentrations do not volatilize Sb more efficiently (Table 2).

It is possible that the mechanisms controlling Sb volatilization vary depending on the environment and microorganisms present. It is likely that Sb volatilization is a complex process that is not solely linked to individual soil and solution parameters and that microbial communities present may likely be a major driving force. Supplementing these experiments with molecular methods may provide valuable insight into the microorganisms responsible for driving Sb volatilization [120]. Supplementing microcosm studies with soil enrichment cultures, similar to studies with sewage [53,59,67], and alluvial soils [78] may yield valuable information on the types of microorganisms that are volatilizing Sb more efficiently. Additionally, using inhibiting agents such 2-bromoethanesulfonat for methanogenesis has been shown to enhance As volatilization by up to four times in rice paddy soils [121]. Performing similar experiments with Sb shed insight into the volatile Sb drivers.

Since little is known about the drivers of Sb volatilization, our work sheds light on Sb volatilization occurrence in a variety of waterlogged soil types, which has been found to produce environmentally relevant amounts of volatile Sb. In effect, our results are comparable to those reported for rice paddy soils. As wetlands comprise a large proportion of the Earth's surface, they may be an environmentally relevant source of Sb to the atmosphere. Future works are required to further understand the role of volatile Sb in the biogeochemical cycle and the impact of their presence in the atmosphere.

**Table 2**
Correlation matrix with Pearson r values of instantaneous volatile Sb fluxes regressed against porewater parameters.

| | Instantaneous Volatile Sb (ng $kg^{-1}$ $d^{-1}$) | |
|---|---|---|
| | **Urunga** | **MRC** |
| DOC | -0.08 | 0.34 |
| pH | -0.08 | 0.43 |
| Eh | -0.41 | -0.44 |
| $SO_4^{2-}$ | -0.41 | -0.41 |
| $NH_4^+$ | -0.22 | 0.23 |
| Mn | -0.33 | -0.4 |
| Fe | -0.25 | -0.4 |
| As | -0.41 | 0.3 |
| Sb | -0.45 | -0.14 |
| Unknown Sb Species | -0.03 | NA |

The asterisk (*) indicates a significant correlation with a $p < 0.05$. NA means not applicable.

## 5. Conclusion

Our work investigated the release, speciation, and volatilization of Sb in organic-rich wetland and Fe-rich floodplain soils by conducting a 27-day microcosm experiment. The release of Sb in organic-rich soils was complex and likely related to an interplay of the S, Mn, and C cycles. In the Fe-rich floodplain soils, Sb fate was related to the reductive dissolution of $Fe^{III}$-oxyhydroxides and subsequent immobilization with sulfide phases. All microcosms released environmentally relevant concentrations of Sb into the porewaters. As these soils were either permanently or periodically waterlogged, the release of Sb may pose a potential risk to the surrounding environment. There was no direct detection of TMSb in soil extracts and porewaters. An unknown species was detected in the porewaters (6 days after waterlogging) and potentially in soil extracts in the Urunga soils. Consequently, the observations highlighted the benefits of conducting further investigations on these unknown species. Poor column recoveries indicated that other unknown Sb species may be present in the porewaters. Volatile Sb was detected from both soil types with the organic-rich soils producing more volatile Sb than the Fe-rich floodplain soils. While no association of Sb volatilization with porewater, soil, or surface water properties could be established, our work highlighted that Sb is volatilized from wetland soils and may be an important source of volatile Sb in the atmosphere.

## Environmental implication

Antimony (Sb) is a ubiquitous, but toxic, contaminant. The fate of Sb in anoxic, waterlogged environments is poorly understood and even less studied are the microbial-mediated transformations of Sb (e.g., methylation and volatilization) although some species are hazardous to human health. The release mechanisms of Sb from the solid to aqueous-phase, and transfer to the atmosphere (volatilization) is largely unknown and understudied but may introduce Sb into the atmosphere and in turn impact its biogeochemical cycle. Investigating the release of Sb and subsequent transformations of Sb in the aqueous and gaseous forms is addressed in this manuscript and is of high importance to better understand the fate and cycling of Sb in the environment.

## CRediT authorship contribution statement

**J.N. Caplettea**: Writing – original draft, Visualization, Validation, Methodology, Investigation, Formal analysis, Data curation; **S.C. Wilsonc**: Writing – review & editing, Investigation, Formal analysis, Conceptualization; **A. Mestrota**: Writing – review & editing, Supervision, Project administration, Methodology, Investigation, Funding acquisition, Conceptualization.

## Declaration of Competing Interest

The authors declare the following financial interests/personal relationships which may be considered as potential competing interests: Susan Wilson reports financial support was provided by UNE Special Studies Program Travel Grant. Adrien Mestrot reports financial support was provided by European Commission Marie Sklodowska-Curie Actions. Adrien Mestrot reports financial support was provided by Swiss National Science Foundation. If there are other authors, they declare that they have no known competing financial interests or personal relationships that could have appeared to influence the work reported in this paper.

## Data availability

Data will be made available on request.

## Acknowledgments

All authors would like to thank the four anonymous reviewers for their helpful, constructive feedback on the improvement of this manuscript. J. Caplette would like to thank M. Bishoff, A. Grimmer, L. Stanisic, A. Weber, and R. Nussbaumer for their help with sample collection and measurements. J. Caplette would like to thank Drs. D. Fisher and T. Chavez-Capilla for their help with HPLC troubleshooting and interpretation and Dr. Candace Chow for editing this manuscript. This work was supported by the Intra-European Fellowship from the People Program (Marie Curie Actions) of the European Union's Seventh Framework Program FP7/2007–2013/under REA grant agreement No. 326736, and the Swiss National Science Foundation (SNSF, nr. PP00P2_163661) to A. Mestrot. S. Wilson received financial support from the UNE Special Studies Program Travel Grant.

## Appendix A. Supporting information

Supplementary data associated with this article can be found in the online version at doi:10.1016/j.jhazmat.2024.134230.

## References

[1] Ali, N., Hussain, A., Ahmed, R., Shamsuri, W.N.W., Shaari, A., Ahmad, N., Abbas, S.M., 2016. Antimony sulphide, an absorber layer for solar cell application. Appl Phys A 122, 23. https://doi.org/10.1007/s00339-015-9542-0.

[2] USGS, 2017. Chapter C of Critical Mineral Resources of the United States - Economic and Environmental Geology and Prospects for Future Supplies (Professional Paper), Antimony.

[3] Arsic, M., Teasdale, P.R., Welsh, D.T., Johnston, S.G., Burton, E.D., Hockmann, K., Bennett, W.W., 2018. Diffusive gradients in thin films reveals differences in antimony and arsenic mobility in a contaminated wetland sediment during an oxic-anoxic transition. Environ Sci Technol 52, 1118–1127. https://doi.org/10.1021/acs.est.7b03882.

[4] Bolan, N., Kumar, M., Singh, E., Kumar, A., Singh, L., Kumar, S., Keerthanan, S., Hoang, S.A., El-Naggar, A., Vithanage, M., Sarkar, B., Wijesekara, H., Diyabalanage, S., Sooriyakumar, P., Vinu, A., Wang, H., Kirkham, M.B., Shaheen, S.M., Rinklebe, J., Siddique, K.H.M., 2022. Antimony contamination and its risk management in complex environmental settings: a review. Environ Int 158, 106908. https://doi.org/10.1016/j.envint.2021.106908.

[5] Nishad, P.A., Bhaskarapillai, A., 2021. Antimony, a pollutant of emerging concern: a review on industrial sources and remediation technologies. Chemosphere 277, 130252. https://doi.org/10.1016/j.chemosphere.2021.130252.

[6] European Chemicals Bureau, 2008. diantimony trioxide (Risk Assessment No. 1309–64–4), European Union Risk Assessment Report.

[7] USEPA, 2014. 65 Water Qual Criteria Pollut Pollut Cl (No 3- 058– 04).

[8] Nakamaru, Y.M., Altansuvd, J., 2014. Speciation and bioavailability of selenium and antimony in non-flooded and wetland soils: a review. Chemosphere 111, 366–371. https://doi.org/10.1016/j.chemosphere.2014.04.024.

[9] Oorts, K., Smolders, E., Degryse, F., Buekers, J., Gascó, G., Cornelis, G., Mertens, J., 2008. Solubility and toxicity of antimony trioxide ($Sb_2O_3$) in Soil. Environ Sci Technol 42, 4378–4383. https://doi.org/10.1021/es703061t.

[10] Wang, X., He, M., Xie, J., Xi, J., Lu, X., 2010. Heavy metal pollution of the world largest antimony mine-affected agricultural soils in Hunan province (China). J Soils Sediment 10, 827–837. https://doi.org/10.1007/s11368-010-0196-4.

[11] Wei, C., Ge, Z., Chu, W., Feng, R., 2015. Speciation of antimony and arsenic in the soils and plants in an old antimony mine. Environ Exp Bot 109, 31–39. https://doi.org/10.1016/j.envexpbot.2014.08.002.

[12] Wilson, S., Lockwood, P., Ashley, P., Tighe, M., 2010. The chemistry and behaviour of antimony in the soil environment with comparisons to arsenic: a critical review. Environ Pollut 158, 1169–1181. https://doi.org/10.1016/j.envpol.2009.10.045.

[13] Bennett, W.W., Hockmann, K., Johnston, S.G., Burton, E.D., 2017. Synchrotron X-ray absorption spectroscopy reveals antimony sequestration by reduced sulfur in a freshwater wetland sediment. Environ Chem 14, 345. https://doi.org/10.1071/EN16198.

[14] Frohne, T., Rinklebe, J., Diaz-Bone, R., Du Laing, G., 2011. Controlled variation of redox conditions in a floodplain soil: Impact on metal mobilization and biomethylation of arsenic and antimony. Geoderma 160, 414–424. https://doi.org/10.1016/j.geoderma.2010.10.012.

[15] Warnken, J., Ohlsson, R., Welsh, D.T., Teasdale, P.R., Chelsky, A., Bennett, W.W., 2017. Antimony and arsenic exhibit contrasting spatial distributions in the sediment and vegetation of a contaminated wetland. Chemosphere 180, 388–395. https://doi.org/10.1016/j.chemosphere.2017.03.142.

[16] Kirk, G., 2004. The Biogeochemistry of Submerged Soils, 1st ed. Wiley. https://doi.org/10.1002/047086303X.

[17] Doherty, S., Tighe, M., Wilson, S., 2017. Evaluation of amendments to reduce arsenic and antimony leaching from co-contaminated soils. Chemosphere 174, 208–217. https://doi.org/10.1016/j.chemosphere.2017.01.100.

[18] Filella, M., Belzile, N., Chen, Y.-W., 2002. Antimony in the environment: a review focused on natural waters I. Occurrence. Earth-Sci Rev 57, 125–176. https://doi.org/10.1016/S0012-8252(01)00070-8.

[19] Guo, X., Wu, Z., He, M., Meng, X., Jin, X., Qiu, N., Zhang, J., 2014. Adsorption of antimony onto iron oxyhydroxides: adsorption behavior and surface structure. J Hazard Mater 276, 339–345. https://doi.org/10.1016/j.jhazmat.2014.05.025.

[20] Leuz, A., Mönch, H., Johnson, A., 2006. Sorption of Sb(III) and Sb(V) to goethite: influence on Sb(III) oxidation and mobilization. Environ Sci Technol 40, 7277–7282. https://doi.org/10.1021/es061284b.

[21] Muller, T., Craw, D., McQuillan, A.J., 2015. Arsenate and antimonate adsorption competition on 6-line ferrihydrite monitored by infrared spectroscopy. Appl Geochem 61, 224–232. https://doi.org/10.1016/j.apgeochem.2015.06.005.

[22] Burton, E.D., Hockmann, K., Karimian, N., Johnston, S.G., 2019. Antimony mobility in reducing environments: the effect of microbial iron(III)-reduction and associated secondary mineralization. Geochim Et Cosmochim Acta 245, 278–289. https://doi.org/10.1016/j.gca.2018.11.005.

[23] Hockmann, K., Tandy, S., Lenz, M., Schulin, R., 2014. Antimony leaching from contaminated soil under manganese- and iron-reducing conditions: column experiments. Environ Chem 11, 624. https://doi.org/10.1071/EN14123.

[24] Reddy, K.R., DeLaune, R.D., 2008. Biogeochemistry of wetlands: science and applications. CRC Press, Boca Raton.

[25] Trace elements in waterlogged soils and sediments. In: Rinklebe, J., Knox, A.S., Paller, M.H. (Eds.), 2017. Advances in trace elements in the environment. CRC Press, Taylor & Francis Group, Boca Raton.

[26] Grob, M., Wilcke, W., Mestrot, A., 2018. Release and biomethylation of antimony in shooting range soils upon flooding. Soil Syst 2, 34. https://doi.org/10.3390/soilsystems2020034.

[27] Hockmann, K., Lenz, M., Tandy, S., Nachtegaal, M., Janousch, M., Schulin, R., 2014. Release of antimony from contaminated soil induced by redox changes. J Hazard Mater 275, 215–221. https://doi.org/10.1016/j.jhazmat.2014.04.065.

[28] Weber, F., Voegelin, A., Kaegi, R., Kretzschmar, R., 2009. Contaminant mobilization by metallic copper and metal sulphide colloids in flooded soil. Nat Geosci 2, 267–271. https://doi.org/10.1038/ngeo476.
[29] Lewińska, K., Karczewska, A., Siepak, M., Szopka, K., Gałka, B., Iqbal, M., 2019. Effects of waterlogging on the solubility of antimony and arsenic in variously treated shooting range soils. Appl Geochem 105, 7–16. https://doi.org/10.1016/j.apgeochem.2019.04.005.
[30] Mitsunobu, S., Takahashi, Y., Terada, Y., Sakata, M., 2010. Antimony(V) incorporation into synthetic ferrihydrite, goethite, and natural iron oxyhydroxides. Environ Sci Technol 44, 3712–3718. https://doi.org/10.1021/es903901e.
[31] Caplette, J.N., Gfeller, L., Lei, D., Liao, J., Xia, J., Zhang, H., Feng, X., Mestrot, A., 2022. Antimony release and volatilization from rice paddy soils: Field and microcosm study. Sci Total Environ 842, 156631. https://doi.org/10.1016/j.scitotenv.2022.156631.
[32] Hockmann, K., Planer-Friedrich, B., Johnston, S.G., Peiffer, S., Burton, E.D., 2020. Antimony mobility in sulfidic systems: coupling with sulfide-induced iron oxide transformations. Geochim Et Cosmochim Acta 282, 276–296. https://doi.org/10.1016/j.gca.2020.05.024.
[33] Burton, E.D., Hockmann, K., Karimian, N., 2020. Antimony sorption to goethite: effects of Fe(II)-catalyzed recrystallization. ACS Earth Space Chem 4, 476–487. https://doi.org/10.1021/acsearthspacechem.0c00013.
[34] Hockmann, K., Karimian, N., Schlagenhauff, S., Planer-Friedrich, B., Burton, E.D., 2021. Impact of antimony(V) on iron(II)-catalyzed ferrihydrite transformation pathways: a novel mineral switch for feroxyhyte formation. Environ Sci Technol 55, 4954–4963. https://doi.org/10.1021/acs.est.0c08660.
[35] Mitsunobu, S., Muramatsu, C., Watanabe, K., Sakata, M., 2013. Behavior of antimony(V) during the transformation of ferrihydrite and its environmental implications. Environ Sci Technol 47, 9660–9667. https://doi.org/10.1021/es4010398.
[36] Liamleam, W., Annachhatre, A.P., 2007. Electron donors for biological sulfate reduction. Biotechnol Adv 25, 452–463. https://doi.org/10.1016/j.biotechadv.2007.05.002.
[37] Chen, Y.-W., Deng, T.-L., Filella, M., Belzile, N., 2003. Distribution and early diagenesis of antimony species in sediments and porewaters of freshwater lakes. Environ Sci Technol 37, 1163–1168. https://doi.org/10.1021/es025931k.
[38] Besold, J., Eberle, A., Noël, V., Kujala, K., Kumar, N., Scheinost, A.C., Pacheco, J. L., Fendorf, S., Planer-Friedrich, B., 2019. Antimonite binding to natural organic matter: spectroscopic evidence from a mine water impacted peatland. Environ Sci Technol 53, 10792–10802. https://doi.org/10.1021/acs.est.9b03924.
[39] Besold, J., Kumar, N., Scheinost, A.C., Lezama Pacheco, J., Fendorf, S., Planer-Friedrich, B., 2019. Antimonite complexation with thiol and carboxyl/phenol groups of peat organic matter. Environ Sci Technol 53, 5005–5015. https://doi.org/10.1021/acs.est.9b00495.
[40] Polack, R., Chen, Y.-W., Belzile, N., 2009. Behaviour of Sb(V) in the presence of dissolved sulfide under controlled anoxic aqueous conditions. Chem Geol 262, 179–185. https://doi.org/10.1016/j.chemgeo.2009.01.008.
[41] Olsen, N.J., Mountain, B.W., Seward, T.M., 2018. Antimony(III) sulfide complexes in aqueous solutions at 30 °C: A solubility and XAS study. Chem Geol 476, 233–247. https://doi.org/10.1016/j.chemgeo.2017.11.020.
[42] Ye, L., Chen, H., Jing, C., 2019. Sulfate-reducing bacteria mobilize adsorbed antimonate by thioantimonate formation. Environ Sci Technol Lett 6, 418–422. https://doi.org/10.1021/acs.estlett.9b00353.
[43] Tella, M., Pokrovski, G.S., 2012. Stability and structure of pentavalent antimony complexes with aqueous organic ligands. Chem Geol 292–293, 57–68. https://doi.org/10.1016/j.chemgeo.2011.11.004.
[44] Tella, M., Pokrovski, G.S., 2009. Antimony(III) complexing with O-bearing organic ligands in aqueous solution: an X-ray absorption fine structure spectroscopy and solubility study. Geochim Et Cosmochim Acta 73, 268–290. https://doi.org/10.1016/j.gca.2008.10.014.
[45] Tella, M., Pokrovski, G.S., 2008. Antimony(V) complexing with O-bearing organic ligands in aqueous solution: an X-ray absorption fine structure spectroscopy and potentiometric study. Mineral Mag 72, 205–209. https://doi.org/10.1180/minmag.2008.072.1.205.
[46] Verbeeck, M., Thiry, Y., Smolders, E., 2020. Soil organic matter affects arsenic and antimony sorption in anaerobic soils. Environ Pollut 257, 113566. https://doi.org/10.1016/j.envpol.2019.113566.
[47] Du, Y., Ramirez, C.E., Jaffé, R., 2018. Fractionation of dissolved organic matter by Co-precipitation with iron: effects of composition. Environ Process 5, 5–21. https://doi.org/10.1007/s40710-017-0281-4.
[48] Newcomb, C.J., Qafoku, N.P., Grate, J.W., Bailey, V.L., De Yoreo, J.J., 2017. Developing a molecular picture of soil organic matter–mineral interactions by quantifying organo–mineral binding. Nat Commun 8, 396. https://doi.org/10.1038/s41467-017-00407-9.
[49] Caplette, J.N., Mestrot, A., 2021. Biomethylation and biovolatilization of antimony. in: Antimony. De Gruyter, pp. 251–274.
[50] Hartmann, L., Craig, P., Jenkins, R., 2003. Influence of arsenic on antimony methylation by the aerobic yeast Cryptococcus humicolus. Arch Microbiol 180, 347–352. https://doi.org/10.1007/s00203-003-0600-1.
[51] Jenkins, R., Craig, P., Goessler, W., Miller, D., Ostah, N., Irgolic, K., 1998. Biomethylation of Inorganic Antimony Compounds by an Aerobic Fungus: Scopulariopsis brevicaulis. Environ Sci Technol 32, 882–885. https://doi.org/10.1021/es970824p.
[52] Jenkins, R., Craig, P., Miller, D., 1998. Antimony biomethylation mixed Cult Micro-Org Anaerob Cond 12, 449–455. https://doi.org/10.1002/(SICI)1099-0739(199806)12:6<449::AID-AOC719>3.0.CO;2-4.
[53] Michalke, K., Wickenheiser, E.B., Mehring, M., Hirner, A.V., Hensel, R., 2000. Production of volatile derivatives of metal(loid)s by microflora involved in anaerobic digestion of sewage sludge. Appl Environ Microbiol 66, 2791–2796. https://doi.org/10.1128/AEM.66.7.2791-2796.2000.
[54] Andrewes, P., Cullen, W.R., Polishchuk, E., 2000. Antimony biomethylation by Scopulariopsis brevicaulis: characterization of intermediates and the methyl donor. Chemosphere 41, 1717–1725. https://doi.org/10.1016/S0045-6535(00)00063-1.
[55] Cutter, G.A., Cutter, L.S., 2006. Biogeochemistry of arsenic and antimony in the North Pacific Ocean: arsenic and antimony cycles. Geochem Geophys Geosyst 7, 1–12. https://doi.org/10.1029/2005GC001159.
[56] Cutter, G.A., Cutter, L.S., Featherstone, A.M., Lohrenz, S.E., 2001. Antimony and arsenic biogeochemistry in the western Atlantic Ocean. Deep Sea Res Part II: Top Stud Oceanogr 48, 2895–2915. https://doi.org/10.1016/S0967-0645(01)00023-6.
[57] Feldmann, J., Hirner, A.V., 1995. Occurrence of volatile metal and metalloid species in landfill and sewage gases. Int J Environ Anal Chem 60, 339–359. https://doi.org/10.1080/03067319508042888.
[58] Hirner, A.V., Feldmann, J., Goguel, R., Rapsomanikis, S., Fischer, R., Andreae, M. O., 1994. Volatile metal and metalloid species in gases from municipal waste deposits. Appl Organomet Chem 8, 65–69. https://doi.org/10.1002/aoc.590080111.
[59] Wehmeier, S., Feldmann, J., 2005. Investigation into antimony mobility in sewage sludge fermentation. J Environ Monit 7, 1194. https://doi.org/10.1039/b509538g.
[60] Bentley, R., Chasteen, T.G., 2002. Microbial methylation of metalloids: arsenic, antimony, and Bismuth. MMBR 66, 250–271. https://doi.org/10.1128/MMBR.66.2.250-271.2002.
[61] Filella, M., 2010. Alkyl Derivatives of Antimony in the Environment. In: Sigel, A., Sigel, H., Sigel, R.K.O. (Eds.), Metal Ions in Life Sciences, 8. Royal Society of Chemistry, Cambridge, pp. 267–301. https://doi.org/10.1039/9781849730822-00267.
[62] Li, J., Wang, Q., Oremland, R.S., Kulp, T.R., Rensing, C., Wang, G., 2016. Microbial antimony biogeochemistry: enzymes, regulation, and related metabolic pathways. Appl Environ Microbiol 82, 5482–5495. https://doi.org/10.1128/AEM.01375-16.
[63] Li, J., Yin, Z., Xu, K., Yan, L., Du, J., Jing, C., Shi, J., 2024. Arsenite S-Adenosylmethionine Methyltransferase Is Responsible for Antimony Biomethylation in Nostoc sp. PCC7120. Environ Sci Technol 58, 1934–1943. https://doi.org/10.1021/acs.est.3c07367.
[64] Andrewes, P., Cullen, W.R., Polishchuk, E., Reimer, K.J., 2001. Antimony biomethylation by the wood rotting fungus Phaeolus schweinitzii. Appl Organo Chem 15, 473–480. https://doi.org/10.1002/aoc.131.
[65] Smith, L., Maher, W., Craig, P., Jenkins, R., 2002. Speciation of volatile antimony compounds in culture headspace gases of Cryptococcus humicolus using solid phase microextraction and gas chromatography-mass spectrometry. Appl Organo Chem 16. https://doi.org/10.1002/aoc.303.
[66] Jenkins, R., Forster, S., Craig, P., 2002. Formation of methylantimony species by an aerobic prokaryote: Flavobacterium sp. Arch Microbiol 178, 274–278. https://doi.org/10.1007/s00203-002-0456-9.
[67] Wehmeier, S., Raab, A., Feldmann, J., 2004. Investigations into the role of methylcobalamin and glutathione for the methylation of antimony using isotopically enriched antimony(V). Appl Organo Chem 18, 631–639. https://doi.org/10.1002/aoc.692.
[68] Yang, H., He, M., 2015. Adsorption of methylantimony and methylarsenic on soils, sediments, and mine tailings from antimony mine area. Microchem J 123, 158–163. https://doi.org/10.1016/j.microc.2015.06.005.
[69] Duester, L., Diaz-Bone, R., Kösters, J., Hirner, A., 2005. Methylated arsenic, antimony and tin species in soils. J Environ Monit 7, 1186. https://doi.org/10.1039/b508206d.
[70] Duester, L., Vink, J., Hirner, A., 2008. Methylantimony and -arsenic species in sediment pore water tested with the sediment or fauna incubation experiment. Environ Sci Technol 42, 5866–5871. https://doi.org/10.1021/es800272h.
[71] Caplette, J.N., Grob, M., Mestrot, A., 2021. Validation and deployment of a quantitative trapping method to measure volatile antimony emissions. Environ Pollut 289, 117831. https://doi.org/10.1016/j.envpol.2021.117831.
[72] Andrewes, P., Kitchin, K.T., Wallace, K., 2004. Plasmid DNA damage caused by stibine and trimethylstibine. Toxicol Appl Pharmacol 194, 41–48. https://doi.org/10.1016/j.taap.2003.08.012.
[73] Dopp, E., Hartmann, L.M., Florea, A.-M., von Recklinghausen, U., Rabieh, S., Shokouhi, B., Hirner, A.V., Rettenmeier, A.W., 2006. Trimethylantimony dichloride causes genotoxic effects in Chinese hamster ovary cells after forced uptake. Toxicol Vitr 20, 1060–1065. https://doi.org/10.1016/j.tiv.2006.01.018.
[74] Jenkins, R., 2011. Biomethylation of Arsenic, Antimony and Bismuth. In: Sun, H. (Ed.), Biological Chemistry of Arsenic, Antimony and Bismuth. John Wiley & Sons, Ltd, Chichester, pp. 145–180. https://doi.org/10.1002/9780470975503.ch7.
[75] Hussain, M.M., Bibi, I., Niazi, N.K., Shahid, M., Iqbal, J., Shakoor, M.B., Ahmad, A., Shah, N.S., Bhattacharya, P., Mao, K., Bundschuh, J., Ok, Y.S., Zhang, H., 2021. Arsenic biogeochemical cycling in paddy soil-rice system: interaction with various factors, amendments and mineral nutrients. Sci Total Environ 773, 145040. https://doi.org/10.1016/j.scitotenv.2021.145040.
[76] Mestrot, A., Feldmann, J., Krupp, E.M., Hossain, M.S., Roman-Ross, G., Meharg, A., 2011. Field fluxes and speciation of arsines emanating from soils. Environ Sci Technol 45, 1798–1804. https://doi.org/10.1021/es103463d.

[77] Mestrot, A., Uroic, M.K., Plantevin, T., Islam, M.R., Krupp, E.M., Feldmann, J., Meharg, A., 2009. Quantitative and Qualitative Trapping of Arsines Deployed to Assess Loss of Volatile Arsenic from Paddy Soil. Environ Sci Technol 43, 8270–8275. https://doi.org/10.1021/es9018755.
[78] Meyer, J., Schmidt, A., Michalke, K., Hensel, R., 2007. Volatilisation of metals and metalloids by the microbial population of an alluvial soil. Syst Appl Microbiol 30, 229–238. https://doi.org/10.1016/j.syapm.2006.05.001.
[79] Wickenheiser, E.B., Michalke, K., Hensel, R., drescher, C., Hirner, A., rutishauser, B., bachofen, R., 1998. Volatile Compd gases Emit Wetl Bogs Lake Cadagno.
[80] Isbell, R.F., 2002. The Australian soil classification, Rev. ed. ed, Australian soil and land survey handbooks. CSIRO Pub, Collingwood, VIC, Australia.
[81] Melvin, S.D., Lanctôt, C.M., Doriean, N.J.C., Carroll, A.R., Bennett, W.W., 2018. Untargeted NMR-based metabolomics for field-scale monitoring: Temporal reproducibility and biomarker discovery in mosquitofish (Gambusia holbrooki) from a metal(loid)-contaminated wetland. Environ Pollut 243, 1096–1105. https://doi.org/10.1016/j.envpol.2018.09.071.
[82] Ngo, L.K., Pinch, B.M., Bennett, W.W., Teasdale, P.R., Jolley, D.F., 2016. Assessing the uptake of arsenic and antimony from contaminated soil by radish (Raphanus sativus) using DGT and selective extractions. Environ Pollut 216, 104–114. https://doi.org/10.1016/j.envpol.2016.05.027.
[83] Ashley, P., Craw, D., Tighe, M., Wilson, N., 2006. Magnitudes, spatial scales and processes of environmental antimony mobility from orogenic gold–antimony mineral deposits, Australasia. Environ Geol 51, 499–507. https://doi.org/10.1007/s00254-006-0346-6.
[84] Doherty, S., Rueegsegger, I., Tighe, M.K., Milan, L.A., Wilson, S.C., 2022. Antimony and arsenic particle size distribution in a mining contaminated freshwater river: Implications for sediment quality assessment and quantifying dispersion. Environ Pollut 305, 119204. https://doi.org/10.1016/j.envpol.2022.119204.
[85] Doherty, S., Tighe, M.K., Milan, L.A., Johannessen, B., Mitchell, V., Hamilton, J., Johnston, S.G., Wilson, S.C., 2021. Long-range spatial variability in sediment associations and solid-phase speciation of antimony and arsenic in a mining-impacted river system. Appl Geochem 135, 105112. https://doi.org/10.1016/j.apgeochem.2021.105112.
[86] Tighe, M., Ashley, P., Lockwood, P., Wilson, S., 2005. Soil, water, and pasture enrichment of antimony and arsenic within a coastal floodplain system. Sci Total Environ 347, 175–186. https://doi.org/10.1016/j.scitotenv.2004.12.008.
[87] Mestrot, A., Ji, Y., Tandy, S., Wilcke, W., 2016. A novel method to determine trimethylantimony concentrations in plant tissue. Environ Chem 13, 919. https://doi.org/10.1071/EN16018.
[88] Reimann, C., Fabian, K., Birke, M., Filzmoser, P., Demetriades, A., Négrel, P., Oorts, K., Matschullat, J., de Caritat, P., 2018. GEMAS: Establishing geochemical background and threshold for 53 chemical elements in European agricultural soil. Appl Geochem 88, 302–318. https://doi.org/10.1016/j.apgeochem.2017.01.021.
[89] Doherty, S., 2021. Long-range spatial variability in sediment associations and solid-phase speciation of antimony and arsenic in a mining-impacted river system. Appl Geochem 12.
[90] Wu, T., Cui, X., Ata-Ul-Karim, S.T., Cui, P., Liu, C., Fan, T., Sun, Q., Gong, H., Zhou, D., Wang, Y., 2022. The impact of alternate wetting and drying and continuous flooding on antimony speciation and uptake in a soil-rice system. Chemosphere 297, 134147. https://doi.org/10.1016/j.chemosphere.2022.134147.
[91] ANZG, 2018. Aust NZ Guidel Fresh Mar Water Qual.
[92] Wan, X., Tandy, S., Hockmann, K., Schulin, R., 2013. Changes in Sb speciation with waterlogging of shooting range soils and impacts on plant uptake. Environ Pollut 172, 53–60. https://doi.org/10.1016/j.envpol.2012.08.010.
[93] Lewińska, K., Karczewska, A., Siepak, M., Gałka, B., 2018. The release of antimony from mine dump soils in the presence and absence of forest litter. IJERPH 15, 2631. https://doi.org/10.3390/ijerph15122631.
[94] Gfeller, L., Weber, A., Worms, I., Slaveykova, V.I., Mestrot, A., 2021. Mercury mobility, colloid formation and methylation in a polluted Fluvisol as affected by manure application and flooding–draining cycle. Biogeosciences 18, 3445–3465. https://doi.org/10.5194/bg-18-3445-2021.
[95] Langmuir, D., 1997. Aqueous environmental geochemistry. Prentice Hall, Upper Saddle River, N.J.
[96] Mitsunobu, S., Takahashi, Y., Terada, Y., 2010. μ-XANES evidence for the reduction of Sb(V) to Sb(III) in soil from Sb mine tailing. Environ Sci Technol 44, 1281–1287. https://doi.org/10.1021/es902942z.
[97] Burton, E.D., Bush, R.T., Sullivan, L.A., 2006. Sedimentary iron geochemistry in acidic waterways associated with coastal lowland acid sulfate soils. Geochim Et Cosmochim Acta 70, 5455–5468. https://doi.org/10.1016/j.gca.2006.08.016.
[98] Hockmann, K., Tandy, S., Lenz, M., Reiser, R., Conesa, H.M., Keller, M., Studer, B., Schulin, R., 2015. Antimony retention and release from drained and waterlogged shooting range soil under field conditions. Chemosphere 134, 536–543. https://doi.org/10.1016/j.chemosphere.2014.12.020.
[99] Burdige, D.J., Nealson, K.H., 1986. Chemical and microbiological studies of sulfide-mediated manganese reduction. Geomicrobiol J 4, 361–387. https://doi.org/10.1080/01490458609385944.
[100] Chadwick, S.P., Babiarz, C.L., Hurley, J.P., Armstrong, D.E., 2006. Influences of iron, manganese, and dissolved organic carbon on the hypolimnetic cycling of amended mercury. Sci Total Environ 368, 177–188. https://doi.org/10.1016/j.scitotenv.2005.09.039.
[101] Li, H., Santos, F., Butler, K., Herndon, E., 2021. A critical review on the multiple roles of manganese in stabilizing and destabilizing soil organic matter. Environ Sci Technol 55, 12136–12152. https://doi.org/10.1021/acs.est.1c00299.
[102] Karimian, N., Johnston, S.G., Burton, E.D., 2021. Reductive transformation of birnessite and the mobility of co-associated antimony. J Hazard Mater 404, 124227. https://doi.org/10.1016/j.jhazmat.2020.124227.
[103] Karimian, N., Johnston, S.G., Burton, E.D., 2018. Iron and sulfur cycling in acid sulfate soil wetlands under dynamic redox conditions: A review. Chemosphere 197, 803–816. https://doi.org/10.1016/j.chemosphere.2018.01.096.
[104] Burton, E.D., Bush, R.T., Johnston, S.G., Sullivan, L.A., Keene, A.F., 2011. Sulfur biogeochemical cycling and novel Fe–S mineralization pathways in a tidally re-flooded wetland. Geochim Et Cosmochim Acta 75, 3434–3451. https://doi.org/10.1016/j.gca.2011.03.020.
[105] Ge, Z., Wei, C., 2013. Simultaneous Analysis of SbIII, SbV and TMSb by High Performance Liquid Chromatography–Inductively Coupled Plasma–Mass Spectrometry Detection: Application to Antimony Speciation in Soil Samples. J Chromatogr Sci 51, 391–399. https://doi.org/10.1093/chromsci/bms153.
[106] Edvantoro, B.B., Naidu, R., Megharaj, M., Merrington, G., Singleton, I., 2004. Microbial formation of volatile arsenic in cattle dip site soils contaminated with arsenic and DDT. Appl Soil Ecol 25, 207–217. https://doi.org/10.1016/j.apsoil.2003.09.006.
[107] Cox, D.P., Alexander, M., 1973. Effect of phosphate and other anions on trimethylarsine formation by candida humicola. Appl Microbiol 25, 6.
[108] Frankenberger, W.T., 2002. Environmental chemistry of arsenic, Books in soils, plants, and the environment. Marcel Dekker, New York.
[109] Wuerfel, O., Thomas, F., Schulte, M.S., Hensel, R., Diaz-Bone, R.A., 2012. Mechanism of multi-metal(loid) methylation and hydride generation by methylcobalamin and cob(I)alamin: a side reaction of methanogenesis: methylation and hydride generation by CH3Cob(III) and Cob(I)alamin. Appl Organo Chem 26, 94–101. https://doi.org/10.1002/aoc.2821.
[110] Mestrot, A., Planer-Friedrich, B., Feldmann, J., 2013. Biovolatilisation: a poorly studied pathway of the arsenic biogeochemical cycle. Environ Sci: Process Impacts 15, 1639. https://doi.org/10.1039/c3em00105a.
[111] Wang, P., Sun, G., Jia, Y., Meharg, A.A., Zhu, Y., 2014. A review on completing arsenic biogeochemical cycle: microbial volatilization of arsines in environment. J Environ Sci 26, 371–381. https://doi.org/10.1016/S1001-0742(13)60432-5.
[112] Mueller, V., Chavez-Capilla, T., Feldmann, J., Mestrot, A., 2022. Increasing temperature and flooding enhance arsenic release and biotransformations in Swiss soils. Sci Total Environ 838, 156049. https://doi.org/10.1016/j.scitotenv.2022.156049.
[113] Vanderstelt, B., Temminghoff, E., Vanvliet, P., Vanriemsdijk, W., 2007. Volatilization of ammonia from manure as affected by manure additives, temperature and mixing. Bioresour Technol 98, 3449–3455. https://doi.org/10.1016/j.biortech.2006.11.004.
[114] Obecnea, W.N., Real, J.G., De Datta, S.K., 1988. Effect of soil texture on nitrogen management on ammonia volatilization and total nitrogen losses. Philipp J Crop Sci 13, 145–153.
[115] Gao, S., Burau, R.G., 1997. Environmental factors affecting rates of arsine evolution from and mineralization of arsenicals in soil. J Environ Qual 26, 753–763.
[116] Frankenberger, W.T., 1994. Chapter 15: Microbial Volatilization of Selenium from Soils and Sediments. in: Selenium in the Environment. CRC Press, pp. 369–389.
[117] De Temmerman, L., Waegeneers, N., Thiry, C., Du Laing, G., Tack, F., Ruttens, A., 2014. Selenium content of Belgian cultivated soils and its uptake by field crops and vegetables. Sci Total Environ 468–469 77–82. https://doi.org/10.1016/j.scitotenv.2013.08.016.
[118] Frankenberger, W.T., 1998. Short communication: effects of trace elements on arsenic volatilization. Soil Biol Biochem 30, 6. https://doi.org/10.1016/S0038-0717(97)00102-8.
[119] Turpeinen, R., Pantsar-Kallio, M., Kairesalo, T., 2002. Role of microbes in controlling the speciation of arsenic and production of arsines in contaminated soils. Sci Total Environ 285, 133–145. https://doi.org/10.1016/S0048-9697(01)00903-2.
[120] Viacava, K., Meibom, K.L., Ortega, D., Dyer, S., Gelb, A., Falquet, L., Minton, N.P., Mestrot, A., Bernier-Latmani, R., 2020. Variability in arsenic methylation efficiency across aerobic and anaerobic microorganisms. Environ Sci Technol 54, 14343–14351. https://doi.org/10.1021/acs.est.0c03908.
[121] Zhang, X., Reid, M.C., 2022. Inhibition of methanogenesis leads to accumulation of methylated arsenic species and enhances arsenic volatilization from rice paddy soil. Sci Total Environ 818, 151696. https://doi.org/10.1016/j.scitotenv.2021.151696.